

INTRODUCTION

Virtually nothing is known about the amount or nature of chromophoric dissolved organic matter (CDOM) in rainwater. Previous studies have only been able to identify less than 50% of the organic compounds in rainwater (Willey et al. 2000). If rainwater CDOM is a large portion of the unidentified fraction, it will likely be the dominant chromophore and fluorophore in rainwater. Humic-like substances are the most probable source of rainwater CDOM and may either be incorporated into precipitation from wind blown soil particles or formed in the atmosphere from oxidation of soot (Decesari et al. 2002). The presence of strong chromophoric humic like compounds in atmospheric waters has profound ramifications with respect to a wide variety of fundamental questions in atmospheric chemistry particularly regarding the attenuation of sunlight and generation or quenching of radicals that affect the oxidizing capacity of the troposphere. Thus, the primary goal of this thesis is to quantify ranges and patterns of variation in the amount and spectral composition of chromophoric dissolved organic matter (CDOM) in rainwater.

Earlier studies demonstrated that storm type and origin can dramatically affect rainwater composition. Significantly higher levels of a variety of analytes (SO_4^{2-} , NO_3^- , DOC, formaldehyde, Cu, and Fe) have been observed in continental rain (cold fronts, low-pressure systems, and local thunderstorms) relative to coastal or marine rain from (coastal storms, hurricanes, tropical storms, winter warm fronts, and El Nino rain) (Willey et al. 2000). In addition to storm origin, season also dramatically impacts rainwater composition. DOC concentrations in continental rain, for example, are significantly higher in summer compared with winter rain, as are hydrogen peroxide and

total iron. Based on these earlier studies, a second goal of this thesis is to determine how storm origin and season affect the amount and spectral quality of rainwater CDOM.

Previous data indicate that CDOM in natural surface waters is extremely photoreactive, even when exposed to short term irradiations with simulated sunlight. There is a significant loss in both the absorbance and fluorescence characteristics of CDOM in natural waters when irradiated under simulated sunlight for six hours (Kieber et al. 1991). One of the major goals of this thesis is to determine the photolability of rainwater CDOM and compare it to the photodegradation of CDOM in natural surface waters. The photochemical reactivity of rainwater CDOM is central to understanding fundamental questions in atmospheric chemistry because it directly impacts free radical concentrations, as well as the wavelength distribution of sunlight reaching earth's surface.

In addition to quantifying how much CDOM is present in rainwater; it would be extremely useful to begin to evaluate its chemical characteristics. The chemical character of CDOM in rainwater reflects its mixed origin and will be examined by UV-vis and EEM spectroscopy, C/N ratios, and nuclear magnetic resonance (NMR). While the absorption coefficient at 300nm has been used as an index of CDOM abundance (Castillo et al. 1999), spectral slopes calculated from log linear least-square regressions of absorption coefficients versus wavelength could convey information about the molecular weight of CDOM. Excitation and emission spectra (EEM) can be employed to discriminate between CDOM types and to gain insight into the structural nature of the chromophores of the rainwater (Blough et al. 1995). Major fluorescence CDOM component peaks have been designated by letters to describe the unknown chemical

composition (Coble 1996). Four peaks will be used to describe rainwater CDOM: where A and C will indicate terrestrial humic-like substances, M is marine humic-like material, and T will indicate the presence of protein-like substances. Carbon and nitrogen ratios will be determined by dissolved organic carbon (DOC) and total dissolved nitrogen (TDN) values. This ratio will help determine what CDOM is made of in rain and natural waters. ^1H NMR is an effective technique for analyzing the structure of macromolecular compounds (Suzuki et al. 2001). Complex signals (broad or sharp lines) can be examined and characteristics such as aromatic absorbance and aliphatic nature can be determined.

In summary, the goals of this thesis are four-fold. 1) Investigate the abundance and patterns of correlation between CDOM properties and other rainwater components including DOC, pH, and inorganic ions. 2) Quantify the photobleaching of CDOM absorbance and fluorescence in authentic rainwater samples collected during different seasons and different storm types. Determine the role of sample matrix on the rate of photobleaching. 3) Determine the quantum efficiency of CDOM photobleaching, defined as the change of absorbance and fluorescence loss per mole (or quantum) of photons absorbed, as a function of wavelength (wavelength-dependent quantum efficiency) to determine which wavelengths of sunlight are most effective at initiating CDOM photobleaching. 4) Evaluate structural characteristics of rainwater CDOM.

EXPERIMENTAL

Sample Collection

Collection of rainwater samples was performed on an event basis at the University of North Carolina at Wilmington rainwater collection site between February 21, 2002 and

August 11, 2003. This time period was necessary in order to define seasonal variations. The rainwater collection site is an open area typical of inland southeastern North Carolina coastal areas, approximately one hectare, surrounded by a turkey oak, wiregrass, and long leaf pine community. Located at 34°13.9'N, 77°52.7'W on the UNCW campus, the rainwater site is approximately 8.5km from the Atlantic Ocean. There are over 15 years of rainwater composition data for this site, which will be useful in interpretation of the data generated and will allow comparison with other locations. Because of the proximity of the sampling location to the laboratory, sample processing can be initiated within minutes of collection, which reduces the possibility of compositional changes between the time of collection and analysis.

Four Aerochem-Metrics (ACM) Model 301 Automatic Sensing Wet/Dry Precipitation Collectors were used to collect event rain samples. One of these ACM containing a 4L muffled Pyrex glass beaker from which samples for pH, inorganic ions, dissolved organic carbon, hydrogen peroxide, organic acids and CDOM were collected and analyzed. The remaining three ACM were used for trace metal sample collection. These consisted of a high density polyethylene (HDPE) funnel connected by Tygon® FEP- lined tubing to a 2.2L Teflon bottle, all cleaned using trace metal clean procedures and protocols (Bruland et al., 1979; Bruland, 1980; Tramantano et al., 1987). Meteorological data including rain amounts, rain duration, time of day, surface temperature, wind speed, wind direction and storm origin were also recorded. Rain events were characterized by E# where E represents rain event and # corresponds to a specific rain event number. Real time precipitation maps were used to define the end of specific rain events, which initiated the sampling process.

Reagents and Standards

All chemicals were obtained from Fisher Scientific or Aldrich Chemical and were reagent grade or HPLC grade unless stated otherwise. A Milli-Q Plus Ultra-pure water system (Millipore, Bedford, MA) provided water ($>18\text{M}\Omega$) for all analysis, dilutions, reagent and standard preparations. Internal NMR stock primary standard was prepared by adding 10mg of 3-(Trimethylsilyl)propionic-2,2,3,3- d_4 acid (98.0%), sodium salt (DDS) to 1.0mL Deuterium oxide (99.96%, D_2O). The primary stock standard (0.01M) was diluted by a factor of ten and 20 μL was added to the sample in D_2O (0.60mL) giving a final DDS concentration of 33 μM in each sample.

Hydrophobic DOM Extraction

Hydrophobic dissolved organic matter, operationally defined here as humic substances, were extracted using C_{18} cartridges (Waters Chromatography, Milford, MA) by the method of Amador et al. (1990). This technique was chosen over conventional methods using XAD resins because C_{18} is more efficient at removing the fluorescent CDOM from rainwater. Amador et al. (1990) reported that C_{18} extraction of humic substances from seawater was between 22 and 84% more effective relative to XAD-2. Kuo et al. (1993) also recovered 83% of an aquatic fulvic acid using C_{18} solid-phase extraction. In addition, Amador et al (1990) found C_{18} extraction better able to retain the UV-visible and fluorescence characteristics of the isolated humic material relative to XAD. Since these were the characteristics of most interest in this study, C_{18} extraction was the most logical choice of an extraction procedure. A second advantage of using C_{18} extraction is that acetonitrile is the eluant rather than 0.1M NaOH. Therefore, any degradation due to high pH is avoided.

C₁₈ cartridges were preconditioned by washing with 2 X 5 mL acetonitrile followed by 2 X 5 mL Milli-Q water. Samples (500mL) for humic extraction were filtered and loaded onto C₁₈ cartridges. The cartridges were washed with 2 X 5 mL of Milli-Q water to remove residual salts and the bound constituents were eluted with 2 X 3 mL of acetonitrile. Samples were pulled through C₁₈ cartridges by the house vacuum with a 5-port manifold, accompanied with a 1 L side-arm flask. Samples were eluted into 25mL muffled round-bottom flasks and concentrated to dryness under reduced pressure (Buchi Rotavapor, Model RE 111, Switzerland). Traces of water were removed under vacuum (Sargent-Welch Model 1400, Skokie, IL).

Inorganic Ion Analysis

Ammonia concentrations were determined by reacting filtered rainwater samples and standards with orthophthaldialdehyde (OPA) in slightly alkaline solutions (pH \approx 9.5), forming a primary amino bond, where amino acids are masked out by sodium sulfite (Holmes et al. 1999) as modified by (Long et al. 2002, unpublished data). Fluorescence of reacted samples were measured at 360nm (excitation) and 440nm (emission) and compared to standards made with ammonium chloride.

Inorganic anions (Cl⁻, NO₂⁻, NO₃⁻, SO₄²⁻) in all samples were measured with suppressed ion chromatography. Samples were analyzed using a Dionex CD25 Conductivity Detector/GP50 Gradient Pump system in conjunction with an AS14A/AG14A Analysis/Guard column and an ASRS – Ultra 4mm anion self-regenerating suppressor flow path. The use of the guard column prolongs peak performance of the analytical column by retaining sample contaminants. In accordance with recommended column operation procedure, a Sodium Carbonate/Sodium

Bicarbonate eluant (0.8M Na₂CO₃/0.1M NaHCO₃) was used.

Samples and standards (200 µL) were injected directly into the guard/analysis column. The conductivity of samples and standards was then measured above that of the carbonate/bicarbonate eluant solution at a flow rate of 1.00mL/min and a suppressor current of 43mV. Standards of 1/20, 1/50, and 1/100 dilutions were prepared from a concentrate stock solution of 0.569mM NaCl, 1.61mM KNO₃, 1.05mM K₂SO₄, 0.193mM NaNO₂. Sample concentrations were calculated from a linear regression standard curve of concentration as a function of conductivity peak area. All calculations are performed automatically with Dionex Peaknet v 6.4 software on a Dell OPTIPLEX GX260 PC.

Dissolved Organic Carbon and Total Dissolved Nitrogen

Rain samples were analyzed for dissolved organic carbon by high temperature combustion (HTC) using a Shimadzu TOC 5000 total organic carbon analyzer equipped with an ASI 5000 autosampler as described in Willey et al. (2000). A primary standard was prepared from 215mg potassium hydrogen phthalate (KHP) dissolved in 100mL of Milli-Q water. A secondary KHP solution was prepared monthly and consisted of ~25g of the KHP primary solution diluted gravimetrically to 250mL with Milli-Q water. Standards in the range of 33 – 400 µM C were made weekly from the secondary KHP stock solution.

Total dissolved nitrogen was measured similarly to the methods described in Alvarez-Salgado et al. (1998). H₂CO measurements were performed using a commercial Shimadzu TOC-5050A coupled to an Antek 9000N nitrogen-specific chemiluminescence detector (Antek Instruments, TX, USA). Potassium nitrate was used as the standard (Merriam et al. 1996). As verification, a Hansel Laboratory Deep Seawater Reference

(Lot # 06-00, Bermuda Biological Station for Research Inc.) was measured. The reference ran at 21.3 ± 0.24 , $n = 10$ with accepted values ranging from 20.5 to 21.5 $\mu\text{M N}$ (W.Chen, Personal Communication).

The samples were injected (75 μL) into the Shimadzu TOC-5050A furnace, filled with a preconditioned Shimadzu catalyst (Al_2O_3 impregnated with 0.5% platinum), at 680°C. The combustion products (CO_2 , $\text{NO}\cdot$, H_2O , etc.) are carried by high purity CO_2 free air through an in-built Peltier cooler at $\sim 1^\circ\text{C}$ (electronic dehumidifier) for removal of water vapor followed by a Shimadzu particle filter (20mm \AA , sub-micron membrane) and finally into the Shimadzu detector cell. After passing through the Shimadzu detector, the combustion gases are routed through a T-piece and into the Antek 9000N detector by pulling a vacuum at the exit of the Antek permeation-tube drier to the lower the pressure within the NO_x/O_3 reaction chamber. This minimizes background luminescence and increases sensitivity (Walsh, 1989). The flow through the Antek 9000N is set to $\sim 75\%$ of the total flow ($=150\text{mL}\cdot\text{min}^{-1}$) by means of an extra-fine Nupro (swage-lock) metering valve (Bristol Valve and Fitting, Bristol UK). The remaining $\sim 25\%$ ($=37.5150\text{mL}\cdot\text{min}^{-1}$) is vented to the atmosphere. This configuration avoids all backpressure problems derived from running both systems in-line.

The dried $\text{NO}\cdot$ is then mixed with O_3 , leading to production of the excited chemiluminescent NO_2 species, which emits quantifiable light energy upon decay to its ground state. Oxygen flow through the ozone generator is set to $\sim 25\text{mL}\cdot\text{min}^{-1}$ and at 0.5 bar pressure. Such low oxygen inflow increases residence time of oxygen in the ozone generator. This enriches the outflow, and enhances the baseline stability. For the TDN levels usually found in seawater ($5\text{-}50\mu\text{M N L}^{-1}$), the Antek 9000N photomultiplier

(PMT) voltage must be set to 800mV, in the range of x10.

The original E451 and Cape Fear River samples went through Hydrophobic DOM Extraction. Extracted samples were then brought back up into small volumes with 10mL Milli-Q. Dilutions of these extracted samples were then made up in triplicates. The remaining volume of the samples was divided up and used for inorganic ion analysis. Extracted CDOM Nitrogen ($\mu\text{M N}$) was calculated by subtracting the inorganic nitrogen (nitrates, nitrites, and ammonia) from the TDN. CDOM Carbon and Nitrogen ratios were calculated between the pre and post-irradiation experiments for the E451 and CFR samples.

Optical Analysis

Samples for absorbance were warmed to room temperature and filtered through 0.2 μm , acid-washed Gelman Supor® polysulfonone filters enclosed in a muffled glass filtration apparatus. Filtered samples were then divided between two muffled test tubes and then used for absorption spectra and fluorescence. Absorbance scans from 240 to 800nm, 2nm slit width, were made using 10cm Suprasil cuvettes on a Cary 1E dual-beam spectrophotometer connected to a micro-computer. Pre-filtered (0.2 μm) Milli-Q water was used in the reference cell. Absorbance measurements at each wavelength (λ) are baseline corrected by subtracting the absorbance at 700nm (Green and Blough 1994). The required corrections are generally less than 0.002 Abs. units. The accuracy and stability of the instruments was determined before and after each sample set using the instrument proprietary performance tests, and NIST-calibrated transmission filters. CDOM absorption coefficients ($a_{\text{CDOM}\lambda}$, m^{-1}) at each wavelength (λ) was calculated according to Kirk, 1994 : $a_{\text{CDOM}\lambda} = 2.303 A_{\lambda} / l$ where A_{λ} is the corrected

spectrophotometer absorbance reading at wavelength λ and l is the optical pathlength in meters (Kirk 1994). A conservative detection limit of 0.046 m^{-1} , corresponding to 0.002 Abs. units on the spectrophotometer, was estimated from repeated scans of Milli-Q water processed as a sample using a 10cm cell. The detection limit corresponds to the absorbance at wavelengths in the range of 350 to 650nm. Spectral slopes were calculated from linear least-square regressions of the plot of $\ln a(\lambda)$ vs. wavelength for the interval between 270 and 350nm and used as a proxy for molecular weight ranges. The spectral slope will decrease with increasing molecular weight.

Samples for fluorescence were treated in the same manner as those for absorbance measurements. Highly absorbing samples were diluted with Milli-Q water to the point where A_{350} (1 cm pathlength) was ≤ 0.02 to minimize inner filtering effects. Excitation-emission matrix (EEM) fluorescence properties are determined on a Jobin Yvon SPEX Fluoromax-3 scanning fluorometer equipped with a 150 W Xe arc lamp and a R928P detector. Although higher resolution is possible, EEMS are generally constructed by using excitation wavelengths from 250 to 500nm (4 nm intervals) and scanning emission from 280 to 550nm (4 nm intervals). The instrument is configured to collect the signal in ratio mode with dark offset using 5nm bandpasses on both the excitation and emission monochromators. The EEMs were created by concatenating emission spectra measured every 5nm from 250 to 500nm at 51 separate excitation wavelengths (Del Castillo et al. 1999). Scans are corrected for instrument configuration using factory supplied correction factors, which are determined essentially as described in Method 1 of Coble et al. 1993. Post processing of scans is performed using FLToolbox 1.91 developed by Wade Sheldon (University of Georgia) for MATLAB® (Release 11). The software eliminates

Rayleigh and Raman scattering peaks by excising portions ($\pm 10\text{-}15$ nm FW) of each scan centered on the respective scatter peak. The excised data is replaced using three-dimensional interpolation of the remaining data according to the Delaunay triangulation method and constraining the interpolation such that all nonexcised data is retained. Following removal of scatter peaks, data were normalized to a daily-determined water Raman intensity (275ex / 303em, 5 nm bandpasses) and converted to Raman normalized quinine sulfate equivalents (QSE) in ppb (Coble et al. 1998). For samples that required dilution, the scatter corrected fluorescence of the diluent Milli-Q was subtracted and the resultant fluorescence values were multiplied by the dilution factor to obtain the intensity for the original, undiluted sample. Replicate scans are generally within 5% agreement in terms of intensity and within bandpass resolution in terms of peak location. Peak locations are labeled as defined in Coble (1996).

EEM Precision Analysis

A precision test was performed on the EEM analysis with two different rainwater samples. These samples were run in triplicates and tested for initial, initial/dark storage, after solar simulator, and after solar simulator/dark storage. Relative standard deviations were determined for all of the peak maxima (Table 1). As a whole, the percentages ranged from 0.18% to 2.44% for the initial and initial/dark storage and 1.01% to 12.34% for the after solar simulator and after solar simulator/dark storage.

Nuclear Magnetic Resonance

Nuclear magnetic resonance (NMR) spectroscopy is an alternative and powerful tool for characterizing rainwater DOC (Aiken et al. 1985). Liquid phase ^1H -NMR were recorded on a Bruker Avance 400 MHz NMR spectrometer. NMR preparations involved

Table 1. 3D Fluoromax precision test with two different rain samples. Relative standard deviations were calculated for each integrated region. Samples were irradiated for 7 hours under a solar simulator. The irradiated samples were tested again after 13 hours in a controlled dark area. The initial samples were kept in a controlled dark area for 24 hours and then retested, SS = solar simulator, dark = controlled dark storage.

Rain Samples	A peak	C peak	Entire Scan	M peak	T peak
Sample 1, initial	0.18%	0.74%	0.31%	0.69%	0.07%
Sample 2, initial	0.68%	2.44%	1.23%	0.68%	0.34%
Sample 1, initial/dark	0.94%	0.54%	0.63%	0.23%	0.71%
Sample 2, initial/dark	0.78%	0.54%	0.44%	0.31%	0.50%
Sample 1, after SS	2.05%	2.74%	3.02%	2.88%	4.93%
Sample 2, after SS	3.33%	1.01%	3.92%	2.41%	9.93%
Sample 1, after SS/dark	3.74%	4.05%	4.58%	4.81%	6.70%
Sample 2, after SS/dark	5.13%	2.24%	5.54%	3.11%	12.34%

adding 0.60mL of D₂O to the completely dried CDOM extract remaining in the 25mL round-bottom flask. The D₂O was swirled around the flask; the mixture was removed with a 5cc syringe (Popper & Sons, NY), and placed into a 5mm NMR tube. Internal standard (20 μL of 0.001 M, DDS) was then added to the sample in the NMR tube. The sample was placed in a sonicator for 5 seconds to assure the internal standard was mixed well with the sample.

An initial ¹H proton experiment (zg30, 64 scans) (Werner 1994) was used to find the resonance of the HDO peak. Due to the large HDO peak, presaturation techniques (power level 20 dB) were used to help eliminate phasing and integration problem. Each sample was then analyzed using a presaturation experiment (zgpr, 8000 scans) where: pulse angle = 30° (P1 = 11.60 μsec), D1 = 3.00 sec, and PL = 20 dB. After the acquisition, the FID was transformed with exponential multiplication (LB = 5). Line Broadening (LB) is a mathematical manipulation of the data that enhances small signals, which may be otherwise lost in the baseline noise. After phasing, the trimethylsilyl peak of DDS was set to zero ppm and set to a height of 10cm.

The following regions were integrated: 10 to 8.5 ppm, 8.5 to 6.5 ppm, 6.5 to 5.0 ppm (D₂O peak), 5.0 (after D₂O peak) to 4 ppm, 4 to 3 ppm, 3 to 2.1 ppm (ACN peak), 2.1 to 0.1 ppm (before internal standard), 0.1 to -0.1 ppm were made to allow for comparison of different natures of extracted CDOM. After integration, the DDS integral was set to one. Regions between 0.1 to 2.1 ppm were defined as the aliphatic protons and regions between 6.5 to 8.5 ppm represented the aromatic protons.

Phasing, calibration, and integration were done identically for all experiments to allow for comparisons of different rain events and for spectral subtraction of photolysis

before and after experiments. The photolysis experiments involved irradiating the water sample for 12 hours under simulated sunlight. Percentages of $^1\text{H-NMR}$ signals recovered after that were determined by subtracting the after irradiation spectra from the before spectra, phasing the difference, and then integrating the spectral subtraction. The 10 to 8.5 ppm region was set to one during integration for the spectral subtractions.

Supporting Data

A Ross electrode with low ionic strength buffers (McQuaker et al., 1983; Boyle, 1986) was used for pH analysis. Hydrogen peroxide concentrations were measured by a fluorescence decay technique (Kieber and Helz, 1986, Kieber et al., 2001). These supporting data will be used to characterize the rain event and to evaluate whether the patterns of variation observed for chromophoric dissolved organic carbon co-vary with any of these analytes. This supporting data will also allow comparison with rain collected elsewhere.

Photochemical Experiments

Controlled photolysis experiments were performed using procedures described in Kieber et al. (1990) and Kieber et al. (2003). Samples were apportioned into quartz flasks or cells with aliquots removed for initial measurements. In each experiment, corresponding samples were placed in a dark controlled temperature cabinet to serve as the control. The light-exposed samples were placed in a constant temperature water bath and irradiated using a solar simulator (Spectral Energy solar simulator LH lamp housing with a 1000 watt Xe arc lamp) equipped with a sun lens diffuser and an AM1 filter to remove unwanted wavelengths. Light measurements at individual cell locations were made with an Ocean Optics SD2000 spectrophotometer connected to a fiber optic cable

terminated with a CC-UV cosine collector. The system was calibrated with a NIST traceable tungsten lamp and data was collected with OOIrrad software. The solar simulator closely mimics the solar spectrum (Figure 1). The calculated solar spectrum (Richiazzi et al. 1998) and the measured solar spectrum at summer solstice were very similar throughout the spectrum. The solar simulator spectrum had slightly less intensity than the other two but the overall trend was the same.

Aliquots were withdrawn at predetermined time intervals for determination of photobleaching of CDOM. Change in CDOM optical properties with time will be used to evaluate photobleaching kinetics. It is expected that most samples will be optically thin and therefore should follow pseudo first-order decreases in CDOM. In these cases, the derived first order rate constants from photodegradation experiments performed on multiple authentic rainwater samples will be used to evaluate how sample matrix influences photobleaching processes.

Quantum Efficiency Experiments

The quantum efficiency, as it relates to photobleaching of CDOM, is defined as the loss of absorbance or fluorescence per mole (or quantum) of photons absorbed. Quantum efficiency is usually a unitless number when the compound of interest can be quantified in molar concentration. However, CDOM optical properties cannot be determined in such units and the quantum efficiency must be expressed as a unit of absorbance or fluorescence per mole of absorbed photons. Apparent quantum efficiency calculations express the efficiency of photochemical transformations in rainwater.

The experiments to determine photobleaching quantum efficiency were carried out with two methods. The first method employed monochromatic light using a 1000 W

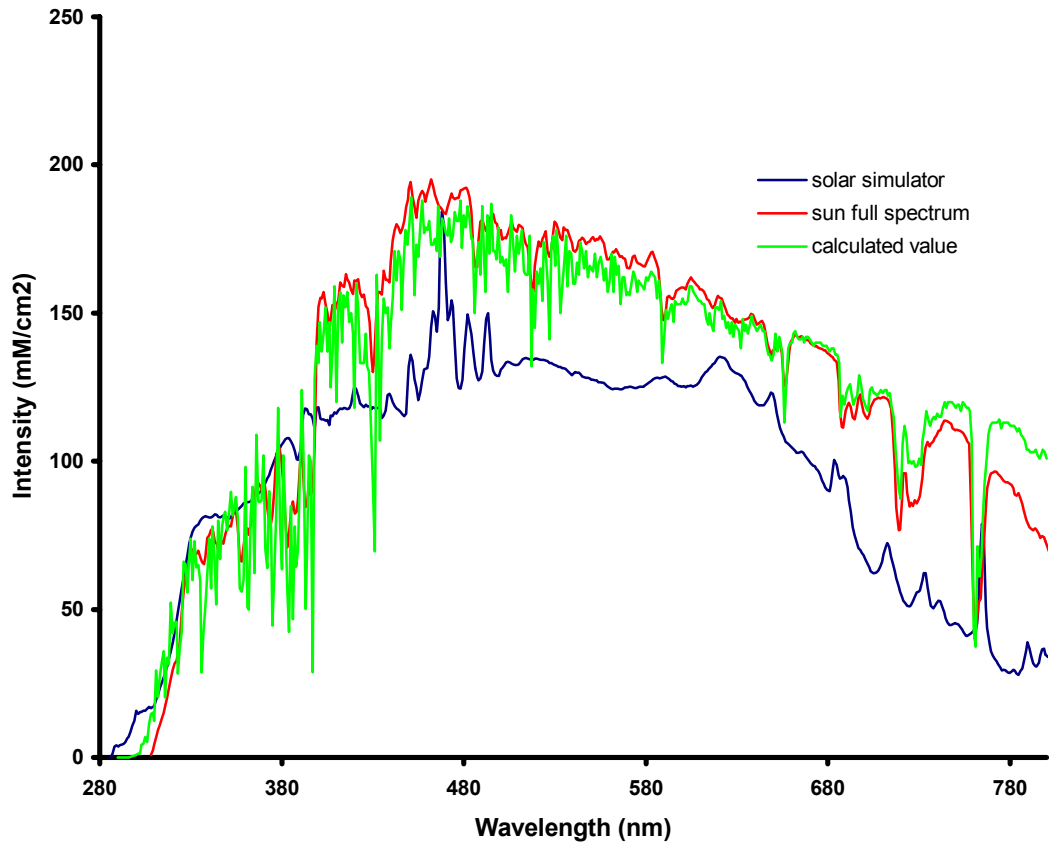


Figure 1. Intensity of the solar spectrum at summer solstice, calculated solar spectrum at solar solstice, and the solar simulator spectrum over wavelengths 280-800nm.

Xe-Hg lamp Spectral Energy Model LH 153 irradiation system equipped with a high-intensity 0.25m grating monochromator (Spectral Energy Corp. model GM 252-20). Light was detected using an international Light IL1700 radiometer (5V bias off) with a calibrated SED033 collector.

Experiments were performed using authentic rain samples that were characterized by EEM, Abs, and DOC. Wavelengths used included 265.2, 300, 313, 365, 404.5, and 435nm. All wavelengths above 400nm had a 400nm long pass filter in place to minimize the effects of second order light. Authentic rain samples were measured initially and at the end of each irradiation. An accompanying dark control was analyzed for each irradiation. Irradiation times for all the wavelengths were for 4 hours. Calculations of the quantum yield using data from the irradiation equipment coupled with conventional actinometric techniques employing Fe(III)oxalate are in described Murov et al. (1993). A potassium ferrioxalate actinometer was used to standardize how much light was being absorbed in the 10cm cell (Hardison et al. 2002). This actinometer was chosen because the quantum yields are well established with its wide range of applicable wavelengths (254-577nm) (Murov et al. 1993). This solution was made in the dark under red light conditions due to the light sensitivity of the actinometer solution (Hardison et al. 2002). A light and dark solution was made to correct for any exposures to unwanted light. From the actinometry solutions, a correction factor resulted in a ratio of 0.539. This correction factor was then applied to all quantum yields (Hardison et al. 2002).

In the second method, the solar simulator was used to determine quantum efficiencies in polychromatic light by placing optical filters on top of sample cells to remove broad wavebands of the light field. The following cut-off filters were used (1%

transmission wavelength given in parentheses) Schott WG335 (313nm), WG360 (348nm), and WG400 (383nm). The differences in transmission among the cut-off filters were used in combination with CDOM absorbance spectra to define four wavebands of rates of photon absorption. Rates of photon absorption (I_{CDOM} in photons $\text{cm}^{-3} \text{h}^{-1} \text{nm}^{-1}$) can be calculated according to Miller (1998):

$$I_{\text{CDOM}\lambda} = I_{-0\lambda} (1 - e^{-K_{d\lambda}l}) F_{\lambda} \frac{A}{V} \quad (\text{Equation 1})$$

Where $I_{-0\lambda}$ is downwelling irradiance in photons $\text{cm}^{-2} \text{h}^{-1} \text{nm}^{-1}$, $K_{d\lambda}$ (cm^{-1}) is attenuation due to a_{CDOM} and water, l is path length in cm, F_{λ} is the ratio of a_{CDOM} and $K_{d\lambda}$, and A and V are irradiated surface area (cm^2) and volume (cm^3) of the cell, respectively. The center of each waveband is defined as the wavelength that divided the area of each respective peak equally.

An apparent quantum yield for photobleaching is determined by dividing the difference in a_{CDOM} photobleaching rates ($\text{m}^{-1} \text{h}^{-1}$) of two adjacent wavebands by the difference in I_{CDOM} integrated over the two wavebands to give units of $\text{cm}^3 \text{m}^{-1} \text{photon}^{-1}$. To account for photobleaching that occurred during the incubation at time t , the average of a_{CDOM} at t and $t-1$ was used in Equation 1. Photobleaching rates were determined from slopes of least squares regressions lines of a_{CDOM} versus time (h). Irradiation times were kept short to ensure that regressions remained linear. An efficiency spectrum was extrapolated from apparent quantum yields by fitting an appropriate modeling equation determined by non-linear least squares regression to the values determined for each waveband. The efficiency spectrum when multiplied by an a_{CDOM} rate of absorption spectrum (Equation 1) yields a spectrum of a_{CDOM} photobleaching rates, which when

integrated over wavelength gives the overall photobleaching rates using only the incident irradiance and the a_{CDOM} absorbance spectrum when a_{CDOM} is the only absorber besides water in the system. This allowed us to determine which wavelengths of sunlight are most effective at initiating CDOM photobleaching.

RESULTS AND DISCUSSION

Rainwater was collected in Wilmington, North Carolina from 125 rain events between February 21, 2002 and August 11, 2003. CDOM, as quantified by absorbance and fluorescence spectroscopy, was detected in all rain events. EEMs spectra (Figure 2) were integrated and surface volume values determined for the A, M, C, T peaks and the entire scan (scatter reducing) (Table 2). Volume weighted averages from integrated values from all of the data for the observed peak maxima A, C, Entire Scan (scatter reducing), M and T were 5440, 1709, 29640, 3623, and 2531 respectively (Table 2). The data presented in Table 2 represent the first detailed data for CDOM in rainwater.

In addition to fluorescence, the CDOM absorbance characteristics were also evaluated. Typical absorbance spectra of continental/coastal and winter/summer rainwater are presented in Figure 3. All absorbance spectra displayed a similar exponential loss of absorbance with wavelength as observed in other natural water samples (Kieber et al. 1990). Spectral slopes were calculated for all rain events from linear least-square regressions of absorbance loss as a function of wavelength. The linear correlation coefficients were generally greater than 0.9 and all were greater than 0.8 corresponding to $P < 0.001$. Average spectral slopes were lower in winter months relative to the summer months (T test, $n = 76$, $p = 0.05$) (Table 3). This suggests winter

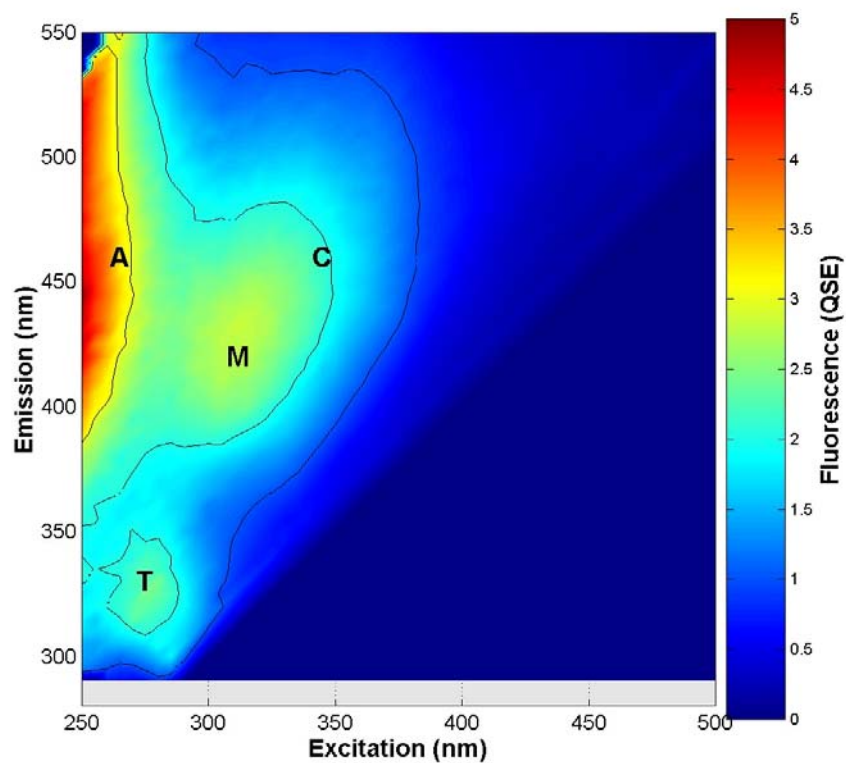
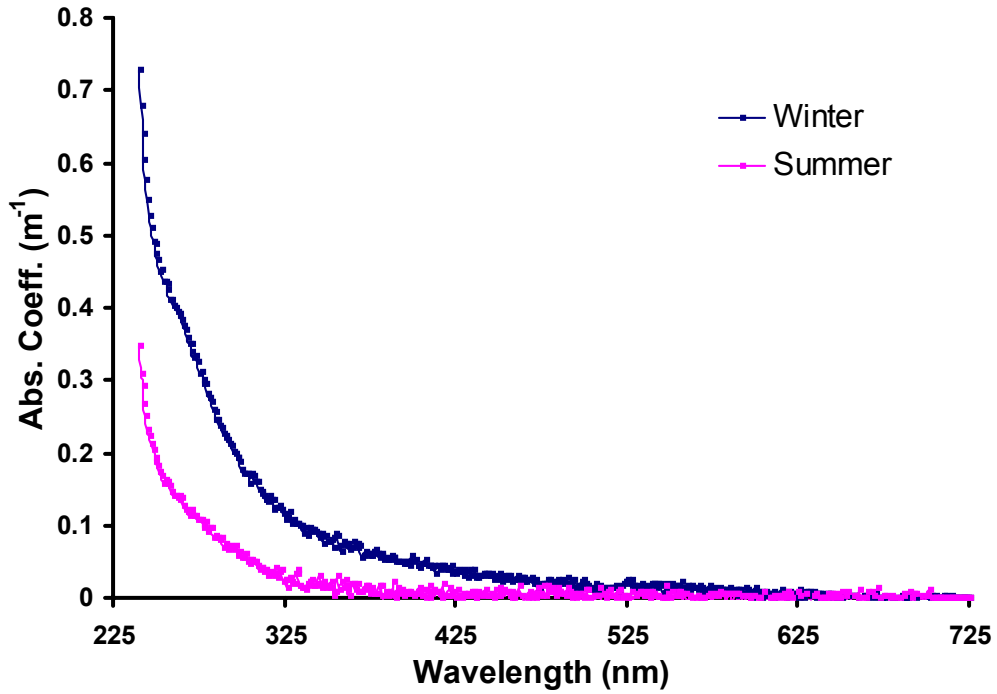


Figure 2. Typical EEM spectra of rainwater. The A, M, C, and T labels are based upon the work of Coble (1996): where A and C indicate terrestrial humic-like substances, M is marine humic-like material and T indicates the presence of protein-like substances.

Table 2. Volume weighted averages from surface volume values from polydata5 fluorescent integrations under each observed peak maxima. The maxima A, M, C, T, and entire scan (scatter reducing) were measured for all rain events collected at Wilmington, NC between February 21, 2002 and August 11, 2003. Average year data represent rain events between February 21, 2002 and February 28, 2003. The A, C, M, T, and entire scan peaks are all relative to the polygon integration program designed by Coble (1996), n = number of samples and amt = rain amount in mm.

	n	Amt. (mm)	pH	DOC (μM)	A peak	C peak	Entire Scan	M peak	T peak
Avg. Year	82	1606	5.30	89	5126	1548	27157	3194	2540
All Data	125	2572	5.08	98	5439	1708	29640	3622	2530
Winter	15	242	4.83	93	7546	1997	37355	4045	2966
Summer	38	938	5.53	80	3970	1217	21799	2869	2010
Coastal	28	678	5.88	50	3709	1007	18853	1728	2284
Cont.	37	756	4.54	151	8904	2983	49933	6704	3402

a. Winter/Summer absorbance plot



b. Coastal/Continental absorbance plot

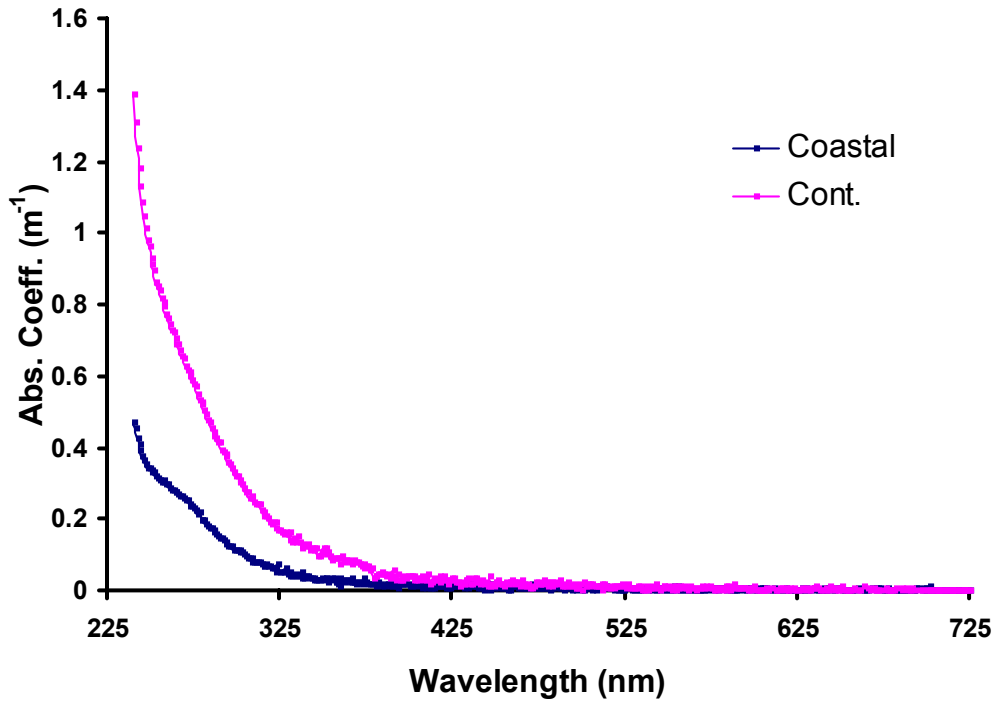


Figure 3-a and b. Typical graphs of winter/summer and coastal/continental rainwater plotted by absorbance coefficient (Abs. Coeff.) and wavelength.

Table 3. Simple average spectral slopes with standard deviations and absorbance coefficients with standard deviations for all rain events and for events broken down by season and storm type.

	Avg. Abs Coeff. (300nm)	Avg. Abs Coeff. (350nm)	Avg. Spectral Slope
All Data	0.67 ± 0.65	0.29 ± 0.35	19.8 ± 5.35
Avg. Year	0.72 ± 0.72	0.34 ± 0.40	18.4 ± 5.33
Winter	0.81 ± 0.89	0.35 ± 0.48	18.6 ± 4.47
Summer	0.42 ± 0.33	0.15 ± 0.10	21.9 ± 4.66
Coastal	0.58 ± 0.80	0.30 ± 0.45	17.4 ± 7.32
Cont.	0.92 ± 0.63	0.37 ± 0.28	20.7 ± 4.62

rain CDOM is comprised of larger molecular weight material possibly explaining why winter rain is more fluorescent.

Correlation Analysis

Correlation analysis was performed on average integrated fluorescence values with other rainwater analytes in order to evaluate patterns of variations between these components and CDOM. Strong correlations ($P < 0.001$) were found among H^+ , NO_3^- , SO_4^{2-} , and all five fluorescence peaks in rainwater, which is consistent with previous correlation analyses of rainwater composition at this site (Kieber et al. 2002). Since H^+ , NO_3^- , and SO_4^{2-} are primarily associated with continental sources, the observed correlations suggest that fluorescent CDOM may also have a predominantly continental source. Additionally, a strong inverse correlation was found between fluorescent CDOM and rain amount indicating that these components are washed out of the atmosphere as rain volume increases. The same correlation was also found between DOC and rain amount ($n = 126$, $p < 0.03$) and suggests that CDOM is not preferentially removed from the atmosphere by rainfall.

The defined fluorescent peak regions were well correlated with each other as well as with Abs. Coeff. at 300nm and 350nm ($n = 126$, $p < 0.001$). This suggests that the fluorescent and absorbing components of rainwater are interrelated and may have similar sources. The optical measurements were also correlated with DOC in rainwater suggesting that CDOM is an important ubiquitous contributor to the organic carbon pool in rain. The correlation between CDOM and DOC is also observed in the covariance of CDOM and DOC both seasonally and by storm type. A strong inverse correlation was found between the absorbance coefficients (300, 350nm) and spectral slope ($n = 126$, $p <$

0.001) and indicates that the least absorbing samples may also have the lowest molecular weight CDOM. A weak correlation was found between spectral slope and any of the fluorescence surface volume values suggesting that CDOM in rainwater maybe composed of a compounds with a broad range of molecular weight.

Seasonality

All rain events were separated into winter and summer seasons in order to determine if there was any seasonality in the amount of CDOM present in rainwater (Table 2). Winter was defined as December 1 to February 28, while the summer season was defined as June 1 to September 30. Volume weighted integrated values were all higher in winter rainwater relative to summer events. Absorbance characteristics of rain events were also separated based on storm origin and seasonality as defined earlier. Average absorbance coefficients were examined at 300 and 350nm. Average absorbance coefficients were higher at both 300 and 350nm during the winter months compared to the summer months indicating there is also more absorbing CDOM present in winter rainwater. There was approximately 40% more fluorescent CDOM in winter A, C, and entire scan regions relative to summer. The M peak had the smallest relative percentage difference between winter and summer rain. This suggests there is not as large a seasonal impact on marine CDOM in rainwater. This is consistent with Willey et al. (2000) who found distinct seasonal differences in terrestrial DOC, but not in marine dominated DOC events.

Impact of Storm Origin

Rain events were subdivided as either coastal or continental in order to determine the influence of storm origin on the amount of CDOM measured in rainwater (Table 2).

Average integrated fluorescence values (A, C, M, T, and entire scan) for continental storms, (which included cold fronts, continental lows and local thunderstorms), were all much larger than those for coastal storms, (which included coastal lows, winter warm fronts, hurricanes and tropical storms,). A higher fluorescent CDOM signal in continental rain suggests terrestrial and/or anthropogenic sources are important contributors to the fluorescence signal of rainwater. One reason the average fluorescence values in continental rainwater are higher is that the rainwater picked up additional CDOM as the air masses are impacted by large landmasses. This is reflected in the substantially lower pH and higher DOC values in continental rain.

Diurnal Variations

All rain events were subdivided based on the time of day during which the rain event occurred in order to determine the diurnal variability of the fluorescent CDOM. Days were divided into four periods from 6am-12pm, 12pm-6pm, 6pm-12am, and 12am-6am local time. Fluorescent CDOM were displayed as the average surface volumes from the entire scans for each time period (Figure 4). The fluorescence decreased gradually over the four periods. The surface volume values were the highest during the morning (6am-12pm) and afternoon (12pm-6pm). Lower surface volume values continued from the evening (6pm-12am) to the early morning (12am-6am). It can be suggested that the fluorescence is the rainwater was degrading while in the atmosphere.

Photochemical Studies

Photochemical experiments were conducted to quantify the photolability of CDOM absorbance and fluorescence in authentic rain samples compared to the

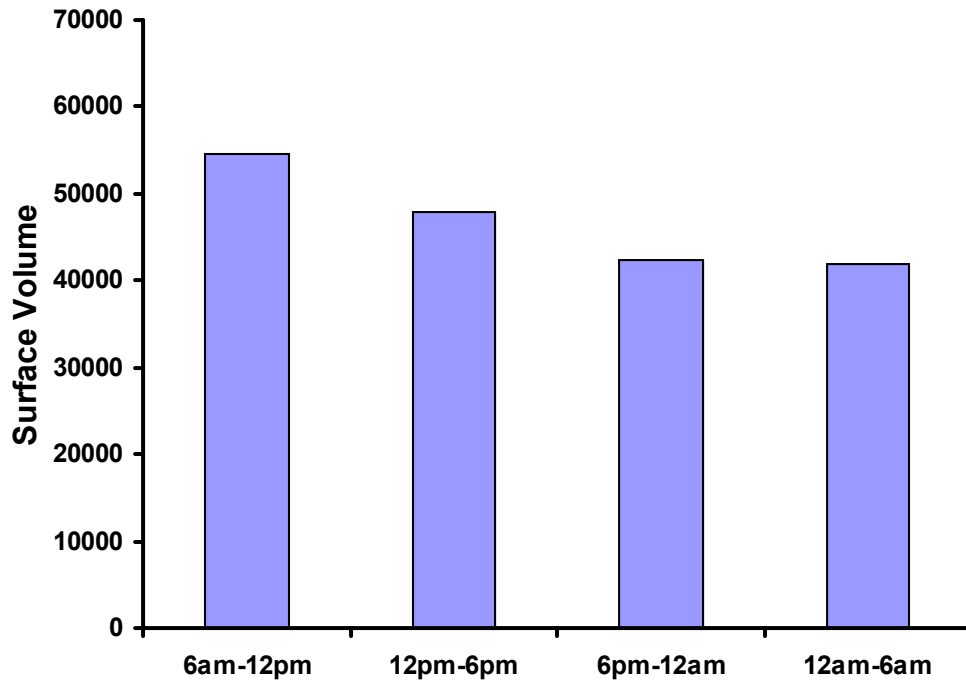


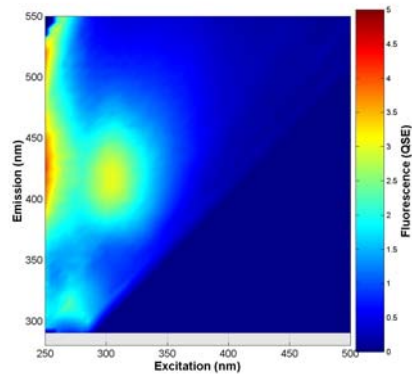
Figure 4. Average surface volumes from EEMs entire scan regions plotted by time of day, n varies from 30 to 35 in each time period.

photolability of estuarine water CDOM in the same geographical region. Authentic rain samples and a Cape Fear River water sample were irradiated for 12 hours under simulated sunlight while the controls remained in the dark throughout the irradiation period. The dark controls had no change in fluorescence after the 12 hour period. There was significant photobleaching of rainwater CDOM fluorescence after 12 hours of light exposure (Figure 5). The percentage of fluorescence lost at each peak maxima was determined for all of rain events. On an average the M peak had the most fluorescence lost and the A peak had the least fluorescence lost after irradiation. On an average between the different seasons and storm types, there were no significant differences concerning the overall fluorescence remaining after the 12 hour irradiation experiments (Table 4).

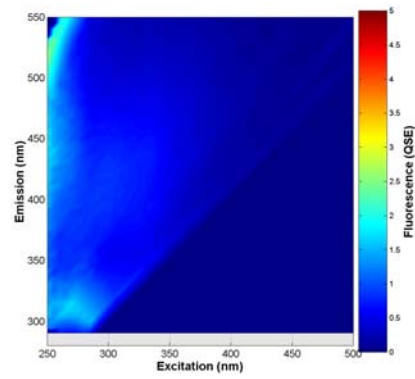
Percentage of fluorescence lost at each peak maxima was also determined for the Cape Fear River sample. There was no change observed in the Cape Fear River dark control. The C peak had the most fluorescence loss and the T peak had the least fluorescence lost after 12 hours under simulated sunlight (Table 4). The fluorescence loss at each peak was very similar to the average fluorescence loss values from the four rain events. The T peak was the only peak that had smaller differences in fluorescence loss.

During these controlled photolysis experiments initial and final absorbance measurements were also taken. The dark control for each rain event had no change over the 12hour irradiation. A typical rain event, E413, before and after absorption spectra were compared with each other (Figure 6). In general, absorbance decreased steadily from 240 to 400nm, past which there was negligible absorbance. The before and after

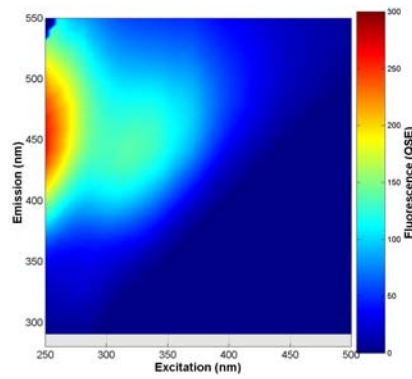
a. E411 before



b. E411 after



c. CFR before



d. CFR after

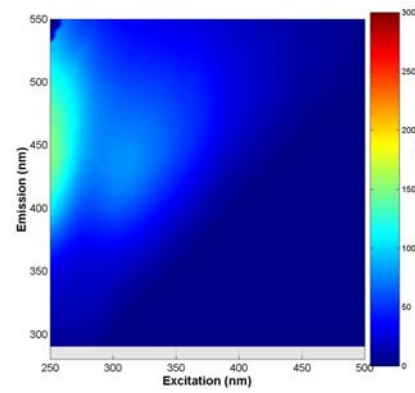
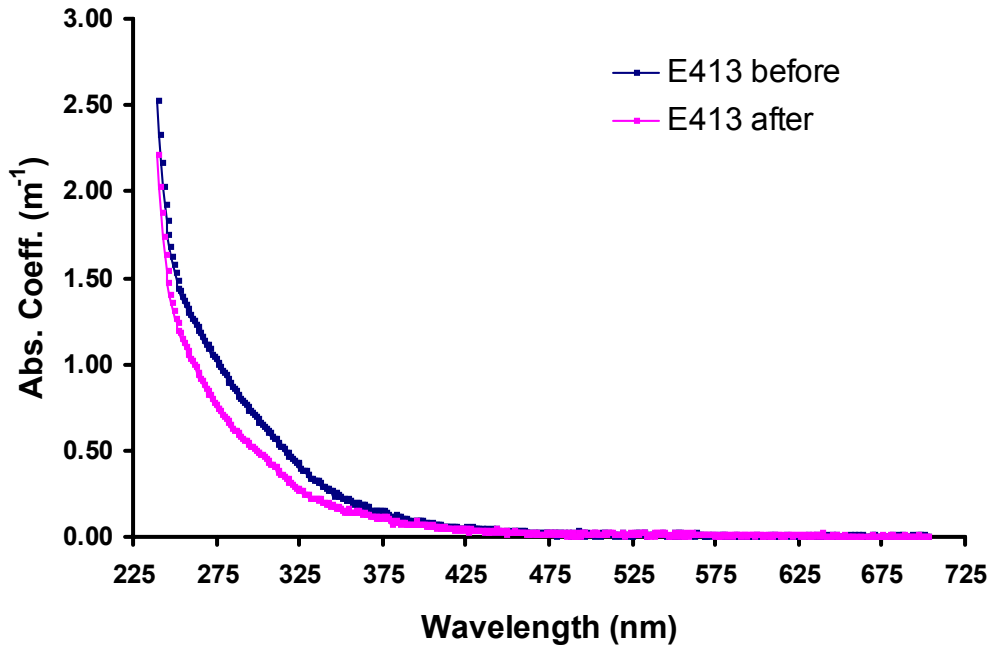


Figure 5-a, b, c, and d. Typical rain event and CFR EEMs before/after 12 hour irradiation under the solar simulator. CFR = Cape Fear River.

Table 4. Percentage of fluorescence loss after 12 hours irradiation. CFR = Cape Fear River.

Samples	A peak (initial)	A peak	C peak (initial)	C peak	M peak (initial)	M peak	T peak (initial)	T peak	Entire Scan (initial)	Entire Scan
E411	8162	49%	2367	55%	5056	68%	3126	29%	40912	52%
E413	15006	42%	5825	47%	8125	59%	3859	35%	79954	48%
E414	4712	17%	1453	19%	2649	33%	7536	39%	33127	30%
E451	3998	40%	1174	52%	3856	70%	2762	47%	25159	51%
Avg. Rain	7970	37%	2705	43%	4922	58%	4321	38%	44788	45%
CFR	592607	41%	238673	49%	244637	42%	42531	20%	2855406	44%

a. E413 before and after absorption spectra



b. E413 difference in absorption spectra

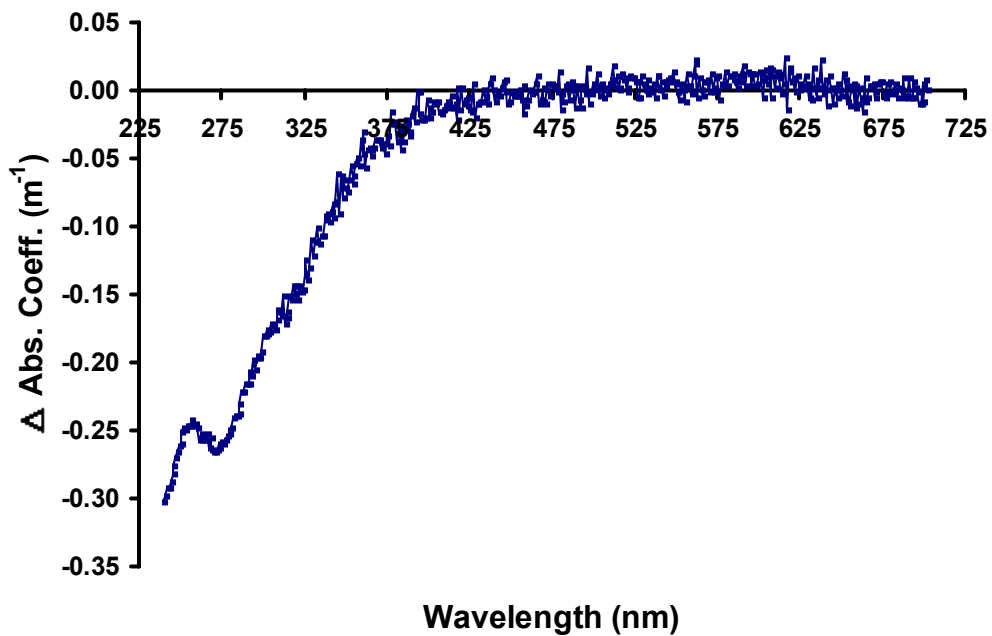


Figure 6-a and b. Typical absorption spectra and difference in absorption spectra before and after irradiation of rain event E413, plotted by absorbance coefficient (Abs. Coeff.) and wavelength.

spectra illustrate that the loss after irradiation is not uniform. The difference between the two spectra shows the loss in light absorbance after irradiation (photobleaching of absorbance). Loss of absorbance from rainwater shifted to the upper end of the UV-A region and the greatest loss was at 275nm (Figure 6). Absorbance coefficient losses at 300 and 350nm were calculated for each photochemical experiment (Table 5). The average absorbance coefficient loss at 300nm was slightly greater than at 350nm. There was no correlation between the decrease in fluorescence and loss of absorbance for the rain events. Seasonal and storm variation had no differences found after the photochemical experiments (Table 6). Spectral slopes were also determined on irradiated rainwater samples. E451 actually showed that its molecular weight increased after irradiation. A possible explanation for this is that the irradiation photoproducted some other material that increased the molecular weight. E414 had no change in its spectral slope, which is due to the contents of the rain event. E414 is different because it has very little fluorescence in the A, C, and M region and has the majority of its fluorescence in the T region.

Initial and final absorbance measurements were obtained for the Cape Fear River sample during the controlled photolysis experiment. The dark control had no change in absorbance during the 12 hour irradiation. Absorbance was found to be a function of wavelength, which was similar to rain (Figure 7). Cape Fear River before and after absorption spectra were compared with each other. In general, absorbance decreased steadily from 240 to 450nm, past which there was negligible absorbance. The before and after spectra show that the loss after irradiation is not consistent, which was similar to typical rain events. Loss of absorbance from the Cape Fear River shifted to the lower end

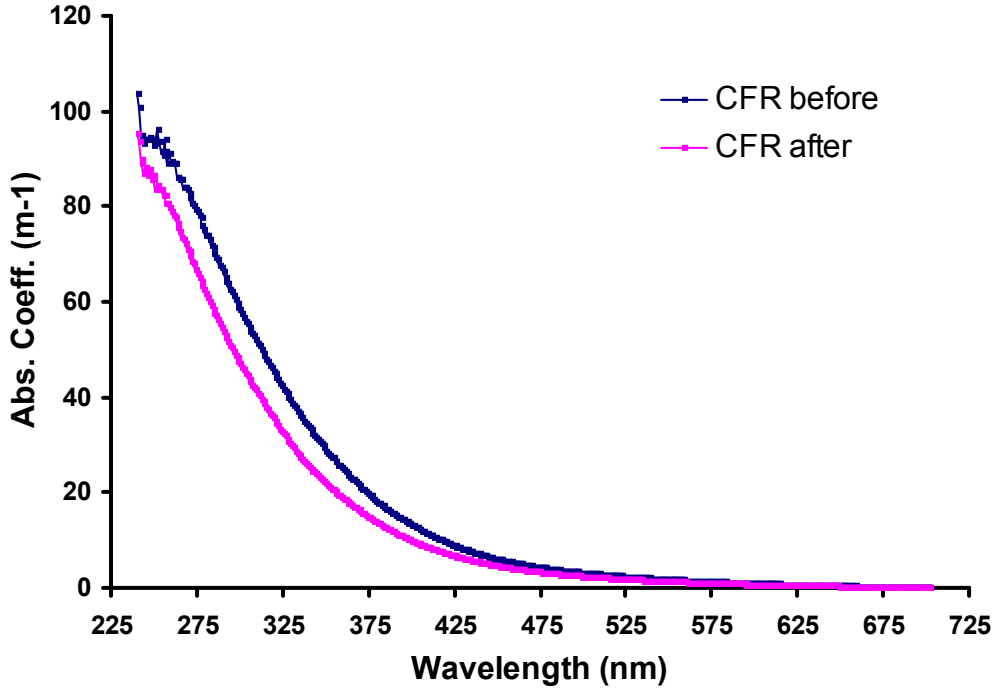
Table 5. Percentages of absorbance coefficients and spectral slopes lost after 12 hours of irradiation. CFR = Cape Fear River.

Samples	Abs Coeff. Lost (300nm)	Abs Coeff. Lost (350nm)	Spectral Slope Before	Spectral Slope After
E411	37%	35%	21	24
E413	27%	32%	20	21
E414	18%	20%	20	20
E451	27%	9%	20	15
Avg. Rain	27%	24%	20	20
CFR	20%	25%	13	15

Table 6. Rain event data for photochemical experiments. N/A = not applicable, cont. = continental.

Sample	Amount (mm)	pH	DOC	Abs.Coeff. (300nm)	Storm type	Season
E411	19	4.76	105	0.55	mixed	winter
E413	20	4.62	32	0.43	cont.	spring
E414	50	4.64	66	0.33	cont.	spring
E451	102	4.39	86	0.28	cont.	summer

a. Cape Fear River before and after absorption spectra



b. Cape Fear River difference in absorption spectra

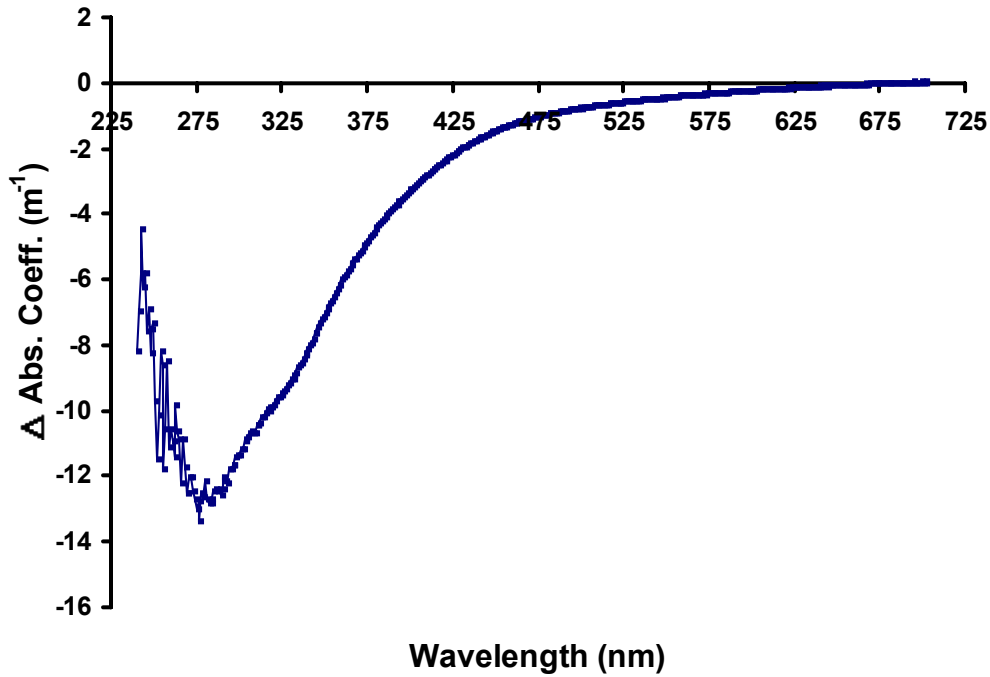


Figure 7-a and b. Absorption spectra and difference in absorption spectra before and after irradiation of Cape Fear River water, plotted by absorbance coefficient (Abs. Coeff.) and wavelength. Note differences in scales compared to Figure 5.

of the UV-B region and the greatest loss was at 285nm (Figure 7), which contrasts the average rainwater sample. The average absorbance coefficient loss at 300nm was less than at 350nm, which was similar to the average rain event (Table 5). Spectral slopes on the irradiated Cape Fear River sample were also determined. The spectral slope increased after irradiation, suggesting photodegradation of higher molecular weight CDOM into lower molecular weight DOM. Both the before and after irradiation spectral slopes were much lower than the average rain events, which suggests that overall the Cape Fear River CDOM is of higher molecular weight than that typically found in rainwater.

C/N Ratios

In order to better understand the mechanism of CDOM photodegradation the C and N content of bulk rainwater and extracted CDOM pre and post irradiation were studied. Photochemical experiments were performed with a summer rainwater sample (pH = 4.39) and a Cape Fear River sample. Initial DOC values were determined for all samples, after which 500mL of each sample was extracted with a C₁₈ solid phase extraction cartridge. CDOM C and N concentrations as well as their relative contribution to DOC and DON were calculated (Table 7). C/N ratios indicate extent of bacterial utilization of organic material. New material has lower C/N ratios preferential because of the use of N by bacteria. Typical marine phytoplankton C/N ratios are $\cong 7$.

There was a much lower C/N ratio in rain initially. The extracted CDOM C did not change upon irradiation, but CDOM N decreased in rainwater and suggests that DON is photodegraded faster than DOC in rainwater. The opposite was found true for the Cape Fear River water sample. Both the CDOM C and N increased, but the CDOM N

Table 7. Carbon/Nitrogen ratios from before/after C₁₈ solid phase extraction cartridge experiments. CFR = Cape Fear River.

Samples	Whole DOC (μM)	Extracted CDOM C (μM C)	% CDOM C (recovered)	Extracted CDOM N (μM N)	CDOM C:N
E451 Pre-Irradiation	53.3	7.4	14%	0.3	25
E451 Post-Irradiation	45.3	7.5	16%	0.2	38
CFR Pre-Irradiation	845.2	188.0	23%	4.7	40
CFR Post-Irradiation	839.8	199.2	24%	8.5	23

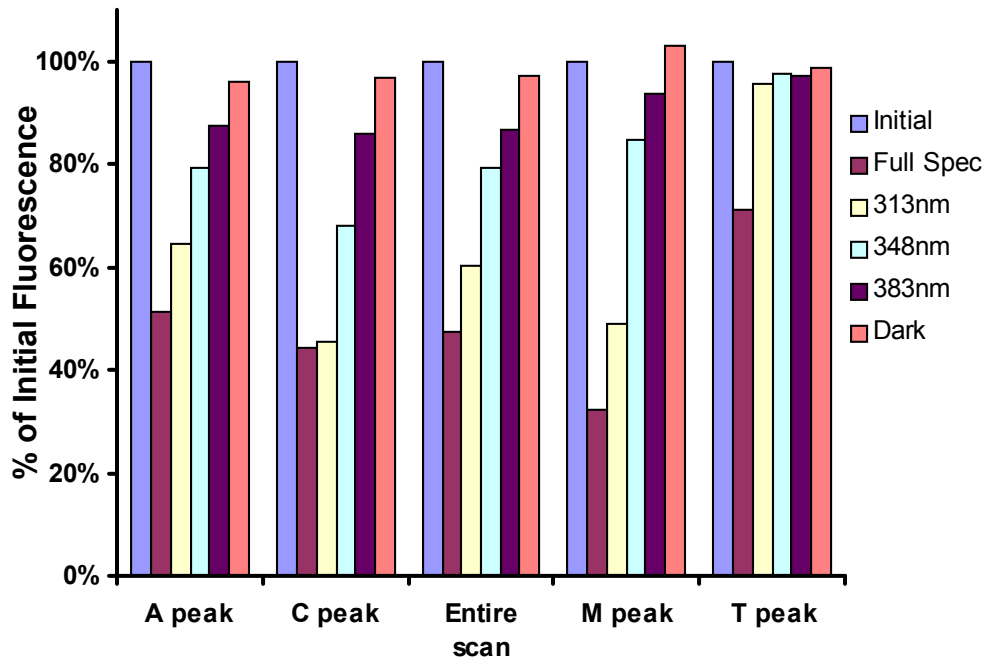
increased more after irradiation and suggests that inorganic N is being transformed into DON during irradiation. Thus, the C/N ratio went down for the CFR. This difference in behavior of C/N ratios suggests that photochemical reactions occurring in rainwater are not the same as in surface waters. The difference in photochemical reactivity may be related to the differing sample matrices or differing chemical composition of the CDOM.

Quantum Efficiency Studies

Several different rain events were photolyzed under the solar simulator equipped with various cut-off filters in order to measure the wavelength regions of the solar spectrum that are most effective at CDOM photodegradation. The photolysis experiments involved isolating four wavebands and irradiating samples for 12 hours (E411, E413, and E414) and 36 hours (E417). The filter number represents the minimum wavelength reaching the sample with all lower wavelengths absorbed by the filter.

The dark control had little or no change in absorbance and fluorescence compared to initial values. EEM spectra of each photolyzed aliquot were plotted after irradiation and subtracted from initial EEM spectra. Percentages of initial fluorescence remaining after the irradiation period were then plotted as a function of fluorescent peak maxima (Figure 8). All four rain events behaved similarly, where samples exposed to the most UV-A and UV-B (full spectrum) had the largest fluorescence lost. As the energy of incoming radiation decreased, the degree of photodegradation also decreased. Greater losses were found with E417, suggesting that longer periods of irradiation increase the degree of CDOM photodegradation. E414 CDOM photodegraded the least, but this sample had the lowest initial fluorescence suggesting its CDOM may have already undergone photodegradation while in the atmosphere before it was collected. The most

a. E411 (12 hours)



b. E413 (12 hours)

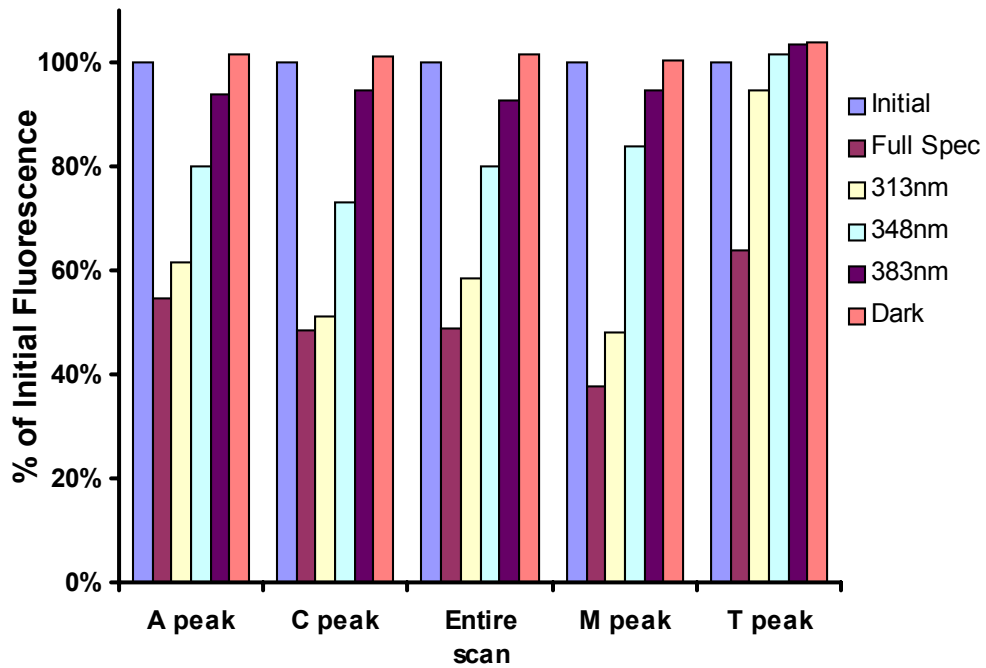
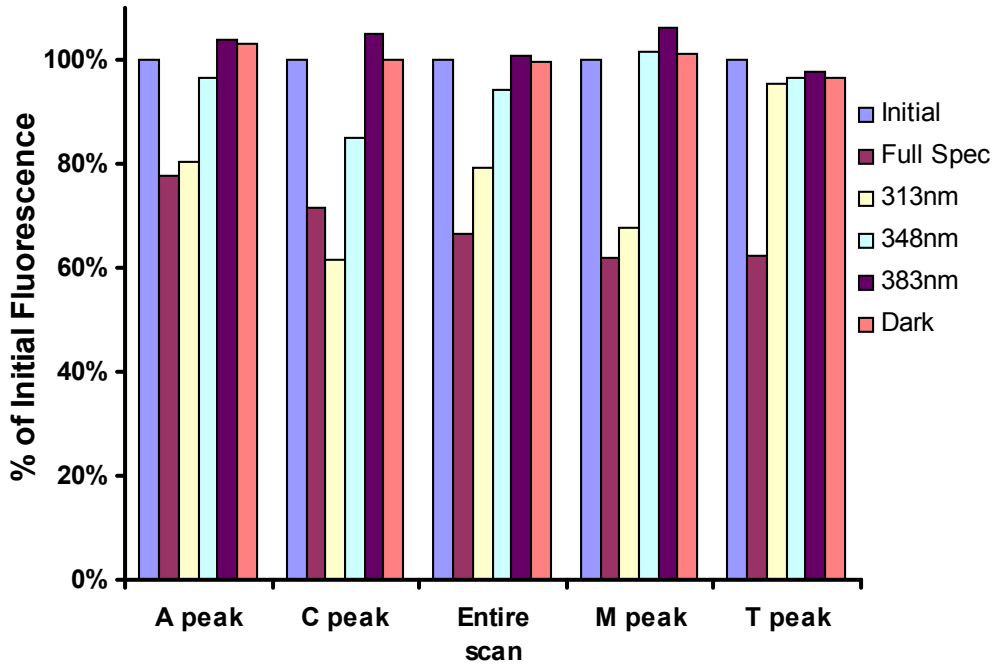


Figure 8-a and b. Percentages of initial fluorescence remaining after 12 hour irradiation using various cut-off filters.

c. E414 (12 hours)



d. E417 (36 hours)

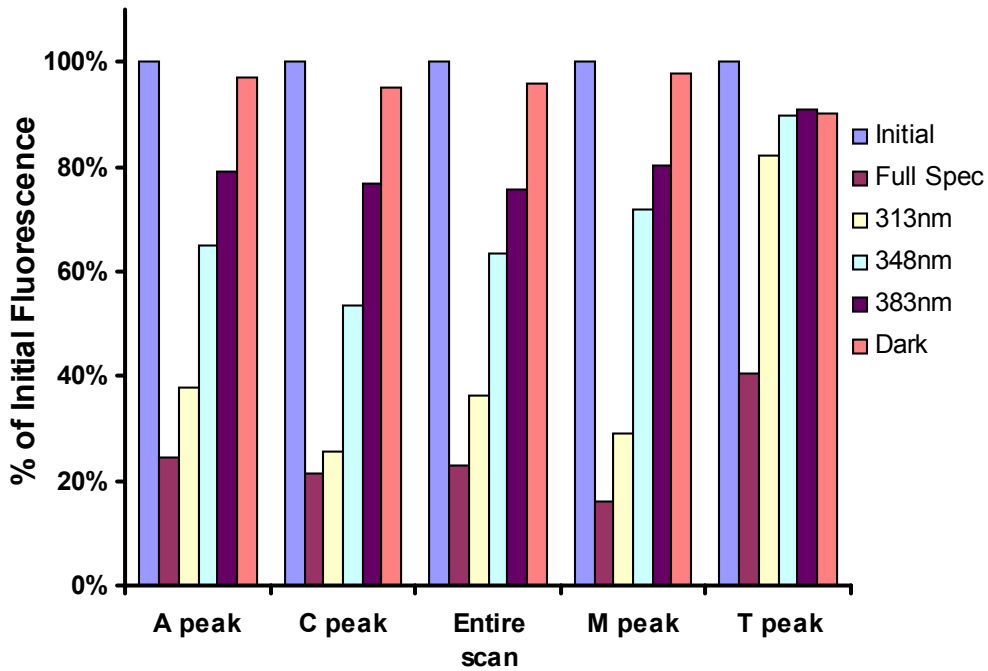


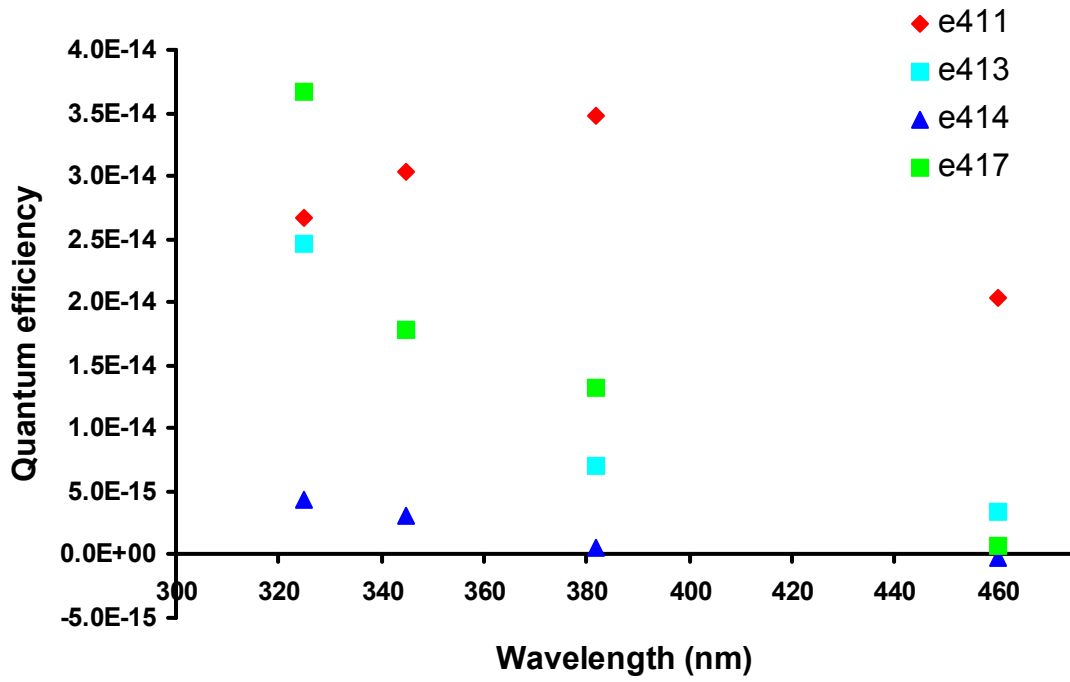
Figure 8-c and d. Percentages of initial fluorescence remaining after 12 hour and 36 hour irradiation using various cut-off filters.

photodegradable peak in all cases at full spectrum was the M peak, while the least amount of fluorescent CDOM destroyed was at the T peak.

Quantum efficiencies or fluorescence loss as a function of photons absorbed from all the rain events were plotted for each EEM fluorescence peak (Figure 9). In general, the efficiency of photodegradation decreased rapidly with increasing wavelength for all peaks. This is most likely because the energy of the irradiation wavelength is decreasing. The most effective wavelength for photobleaching rain event E411 however occurred at 382nm. A possible explanation for E411 having a red shifted efficiency spectrum is because it has significant less initial CDOM fluorescence relative to the other rain events studied.

In addition to solar simulator experiments with cut-off filters, one rainwater sample was also irradiated with monochromatic light. Again, dark controls had no change in fluorescence during the irradiation periods. Quantum efficiency values for fluorescence photobleaching by monochromatic light are presented in Figure 10. As in the polychromatic quantum efficiency experiment, maximum efficiency for all three peaks was observed in the UV-B region after which it declined reaching a minimum at 435nm. However, the photobleaching of fluorescent CDOM with irradiation at 265nm was much less efficient for all peak regions. The peak wavelength for photobleaching for peaks C and M are very similar to their maximum excitation wavelengths. This phenomenon has been observed earlier for the photobleaching of CDOM in natural waters (Del Vecchio et al. 2002). The A peak maximum, in contrast, is red shifted well past its peak excitation wavelength of 260nm. This suggests the mechanism for photodegradation of the A peak CDOM is somewhat different from the C or M peaks and

a. A peaks



b. C peaks

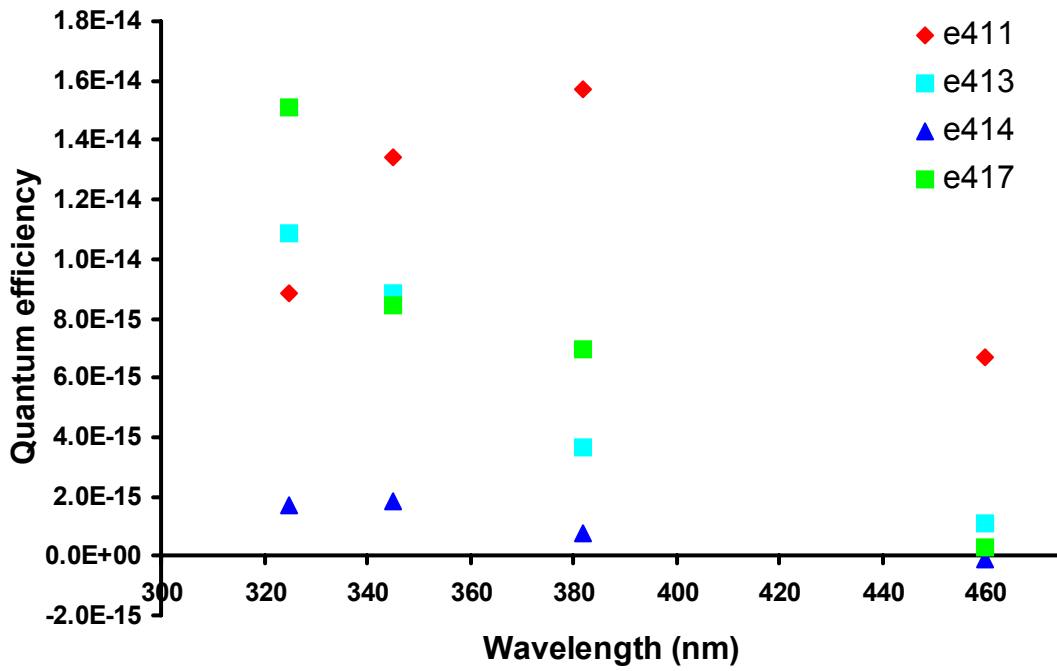
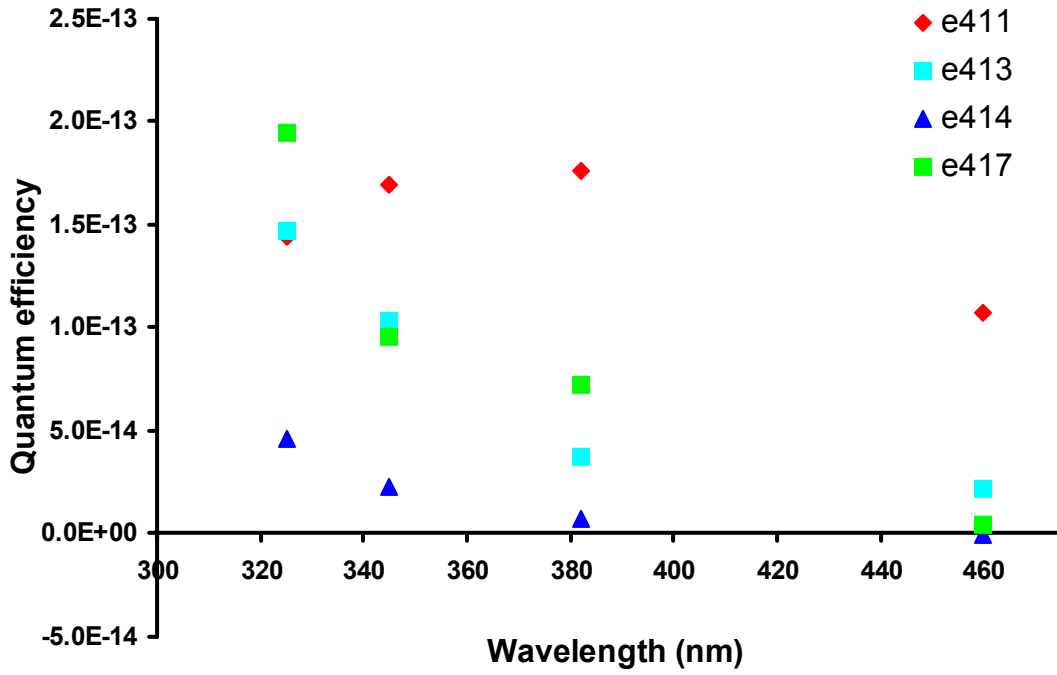


Figure 9-a and b. Quantum efficiency results for A and C peaks.

c. Entire scan peaks



d. M peaks

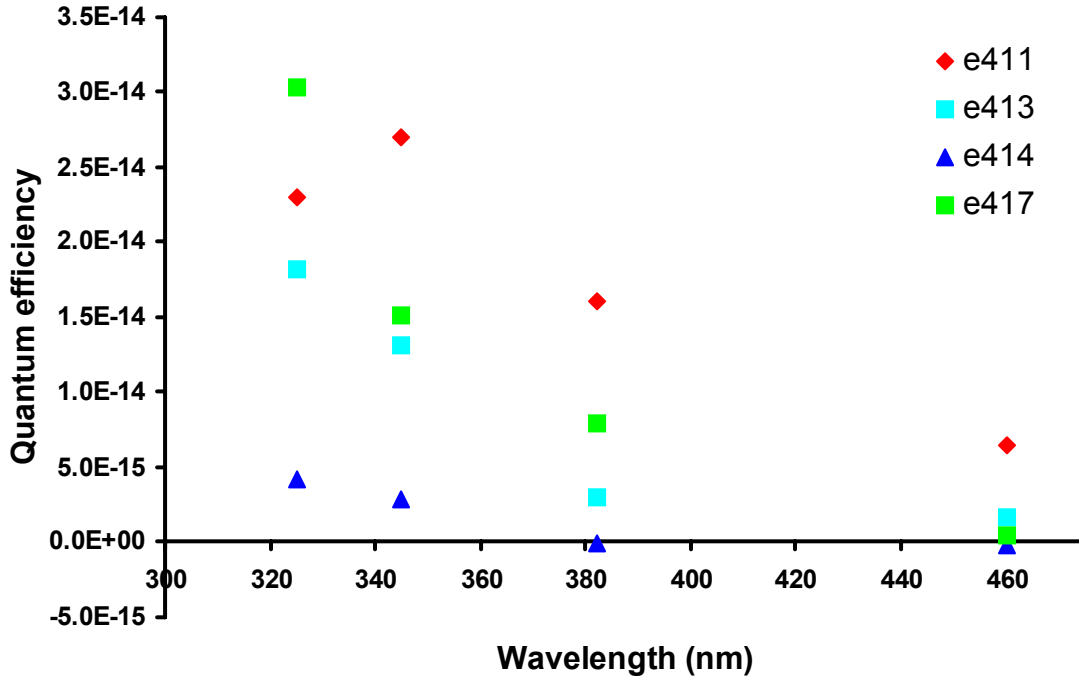
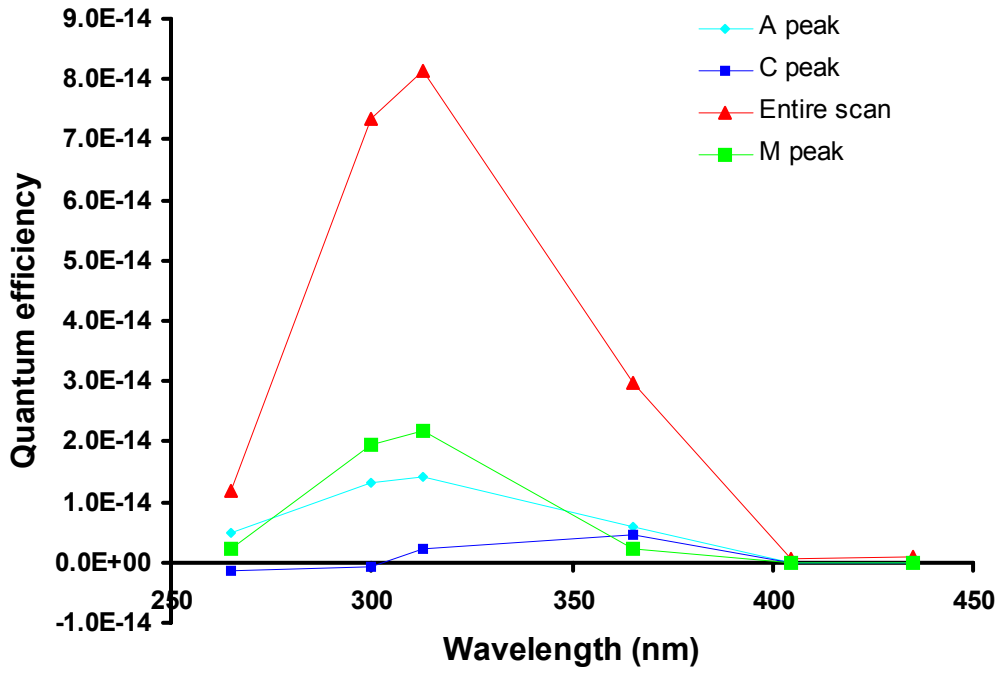


Figure 9-c and d. Quantum efficiency results for entire scan and M peaks.

a. Quantum efficiency plot with all peaks



b. Quantum efficiency plot without entire scan peak

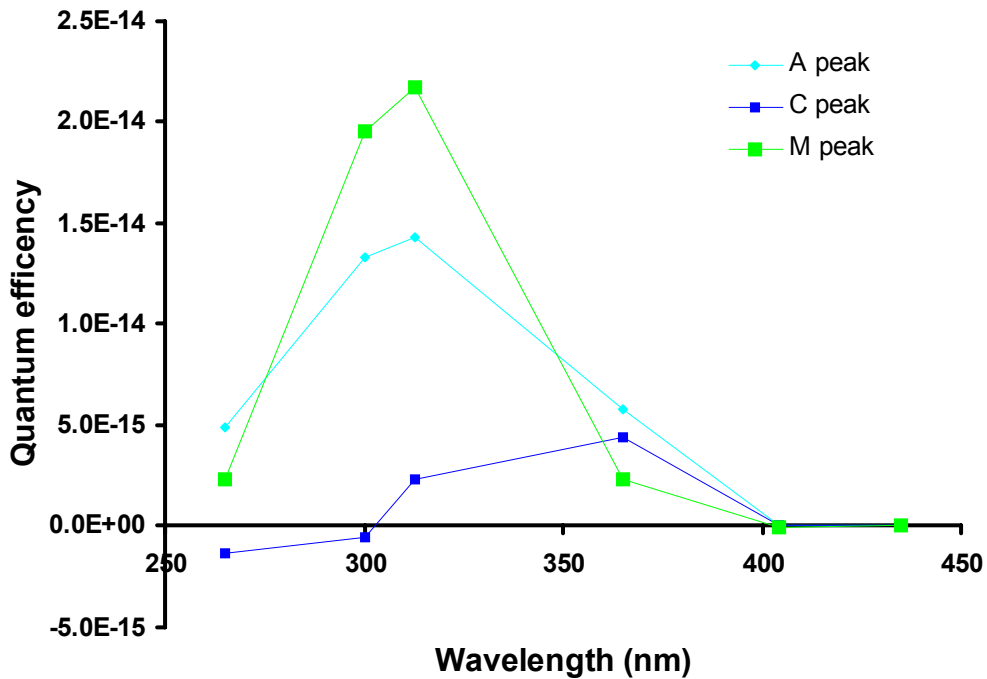


Figure 10-a and b. Quantum efficiency results for the single wavelength experiments. The A, C, M, and entire scan peak regions were plotted at 265.2, 300, 313, 365, 404.5, and 435nm.

natural water CDOM.

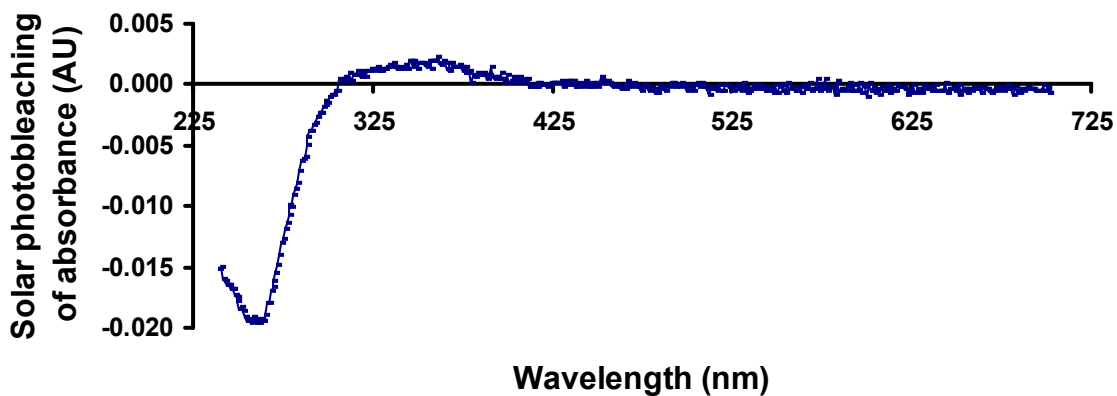
In addition to the fluorescence loss from the monochromatic light, absorbance measurements were recorded before and after the irradiation periods. Three different spectra were compared to examine the photobleaching from each wavelength (Figure 11). The amount of absorbance lost at each wavelength decreases from 265.2 to 435nm, resulting from photobleaching shifting from the UV-A to the UV-B and then to the PAR region (Table 8). The maximum wavelength absorbance lost also showed shifting from 265.2 to 435nm, which resulted from the monochromatic light burning holes in the fluorescent CDOM in the EEMs plots. The monochromatic experiments behaved similarly, where samples exposed to most UV-A and UV-B light had the largest absorbance lost, which was similar to the fluorescence. As the energy of the monochromatic irradiation decreased, the amount of absorbance lost also decreased.

Nuclear Magnetic Resonance Studies

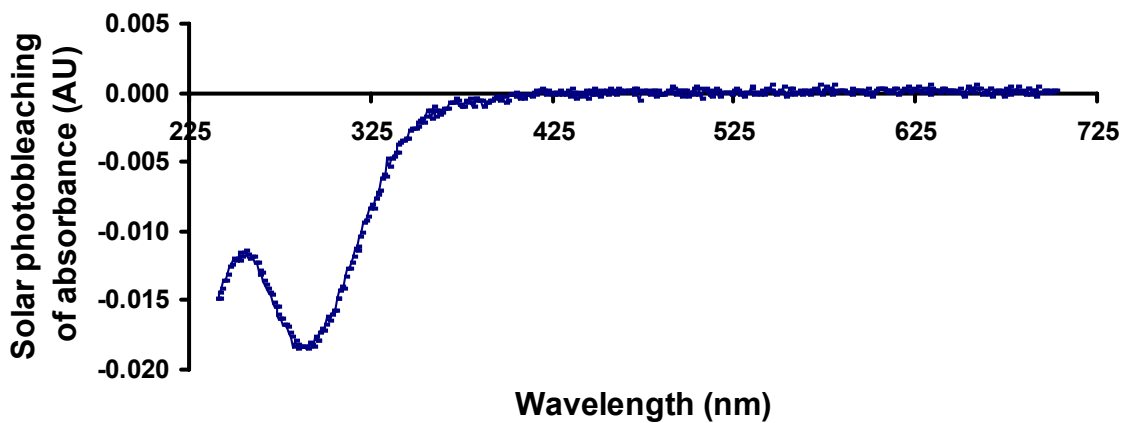
NMR spectroscopy is an alternative and powerful tool for characterizing rainwater DOC. Initially, an NMR spectrum of the DDS internal standard in D₂O was obtained to optimize DDS concentration and presaturation experimental parameters (Figure 12a). Hydrophobic CDOM in rain samples, as well as a Milli-Q blank, was extracted on a C₁₈ solid phase cartridge, eluted with acetonitrile, concentrated to dryness, and dissolved in D₂O containing 1 μM DDS, for ¹H NMR analysis. Comparison of the spectra from the blank (Figure 12b) with a rainwater extraction (Figure 12c), where the internal standard signal at 0 ppm is set to 10cm, showed that there was very little signal due to the extraction method alone.

The internal standard also made it possible to compare different rain events with

a. 265.2nm



b. 300nm



c. 313nm

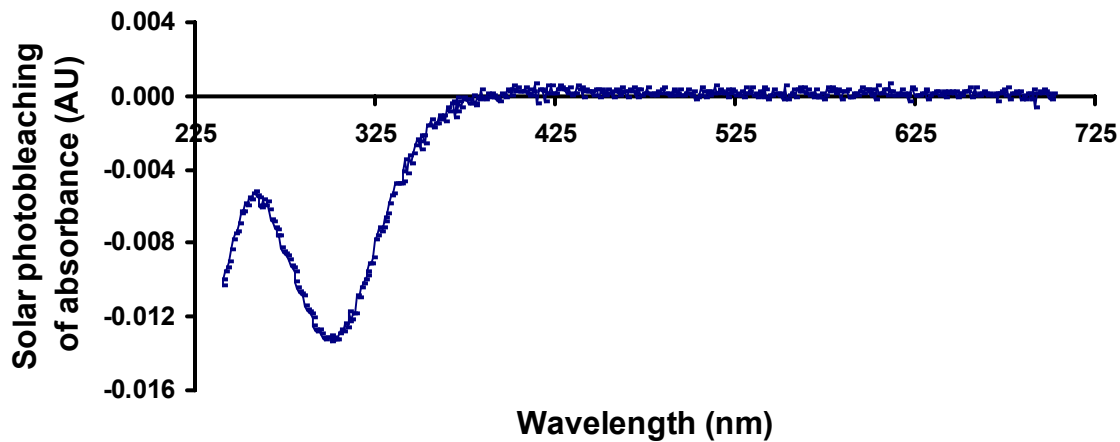
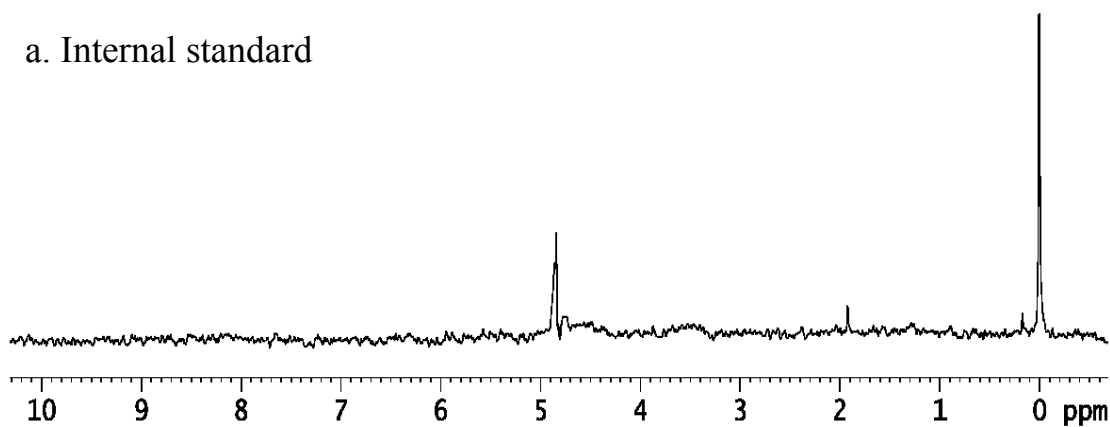


Figure 11-a, b, and c. Difference in absorption spectra before and after monochromatic irradiation at 265.2, 300, and 313nm.

Table 8. Quantum efficiency absorbance loss for E417 after single wavelength irradiation. Examples of λ maximum Abs. loss shown in Figure 11.

Irradiation λ (nm)	Amount of Abs. loss	λ Maximum Abs. loss (nm)
265.2	-0.0197	262
300	-0.0185	290
313	-0.0130	301
365	-0.0044	345
404.5	-0.0011	385
435	-0.0008	411

a. Internal standard



b. Blank extraction



c. E414

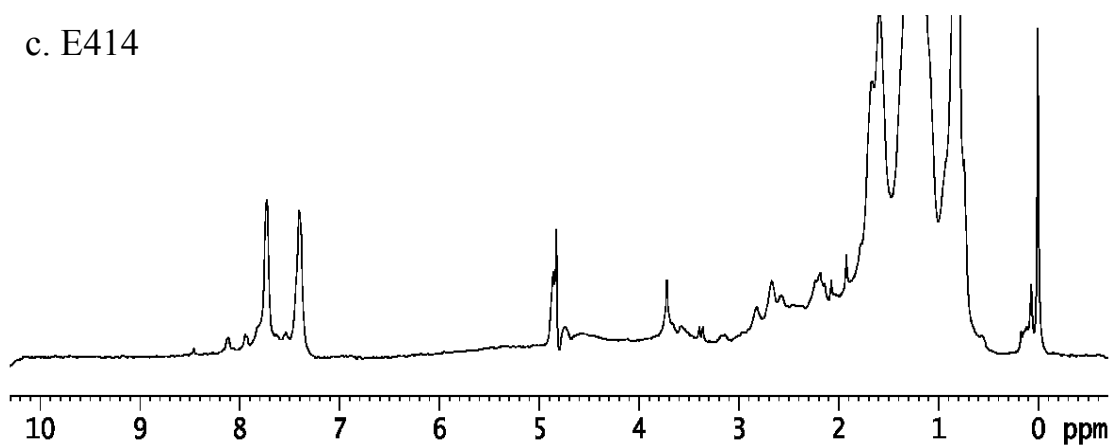


Figure 12-a, b, and c. ^1H NMR presaturation spectra of the internal standard, blank extraction and extraction of CDOM from rain event E414.

each other and with an estuarine sample, and for comparison between the before and after irradiation experiments for the rain events. Rain events E414, E451, and the Cape Fear River sample are compared in Figure 13 and show that the majority of the CDOM of each rain sample is in the aliphatic region (0.1 to 3.0 ppm). E414 has larger peaks in the aliphatic region compared to E451, indicating the presence of more saturated alkyl chains. E414 also has a distinct pattern in the aromatic region, which is not present in the E451 rain sample.

The Cape Fear River spectra were obtained from 50mL of filtered river water versus 500mL used for rain events, since there is such a greater concentration of DOC in the river water. The Cape Fear River spectra displays larger broader peaks in the aromatic and aliphatic regions, which indicates a greater complexity or higher molecular weights of the DOC in river water compared to rain water. Larger molecular weight DOC was also indicated for the Cape Fear River by the smaller spectral slopes obtained from UV-vis analysis of CFR vs. rain samples.

The photochemical lability of CDOM was also investigated by nuclear magnetic resonance. ^1H -NMR presaturation experiments were conducted on before and after 12 hour irradiation experiments with different authentic rain samples. Percentages of integral regions from ^1H -NMR experiments from rain samples from before and after 12 hours under the solar simulator were compared to integrations from a Cape Fear River sample (Figure 14). The rain events did not show much change after irradiation within the regions 10 to 2.1 ppm, but did show greater loss in the region 2.1 to 0.1 ppm. E451 also displayed loss in the region 3 to 2.1 ppm, while 414 showed no change in that region. Irradiation possibly caused the loss of alkyl chains or alkyl aldehydes, such as

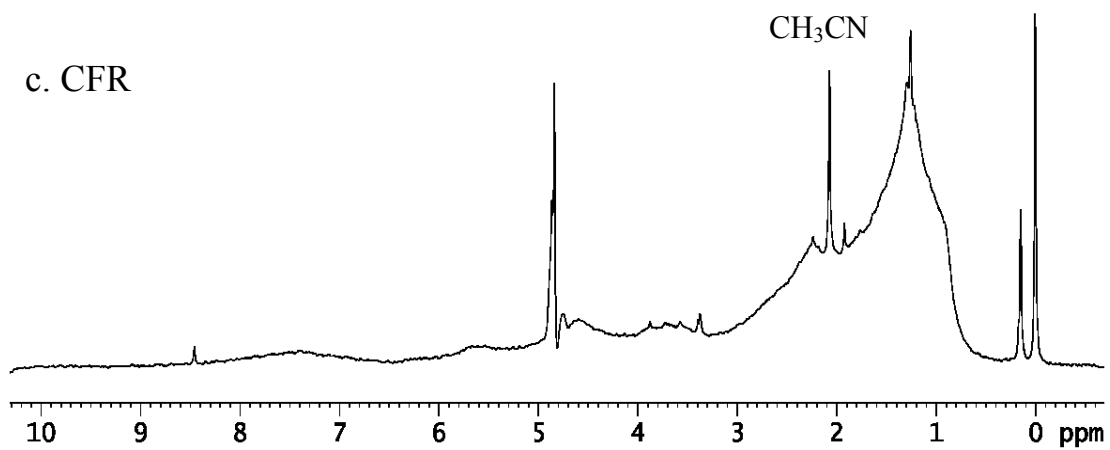
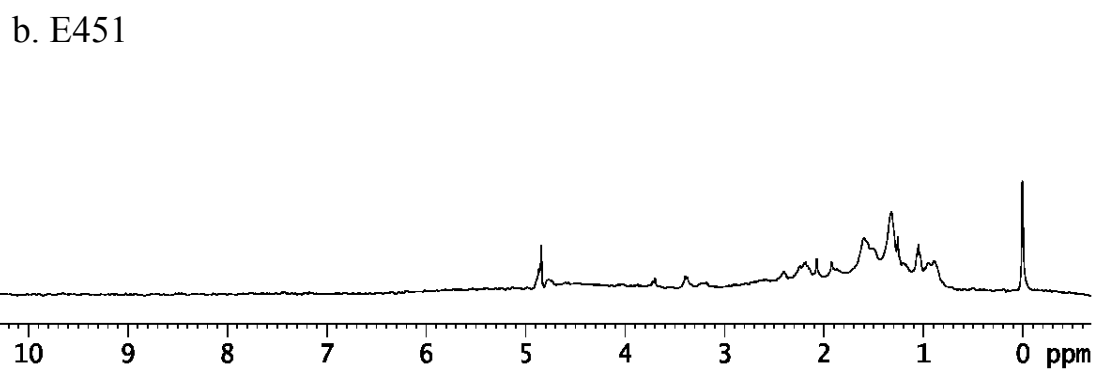
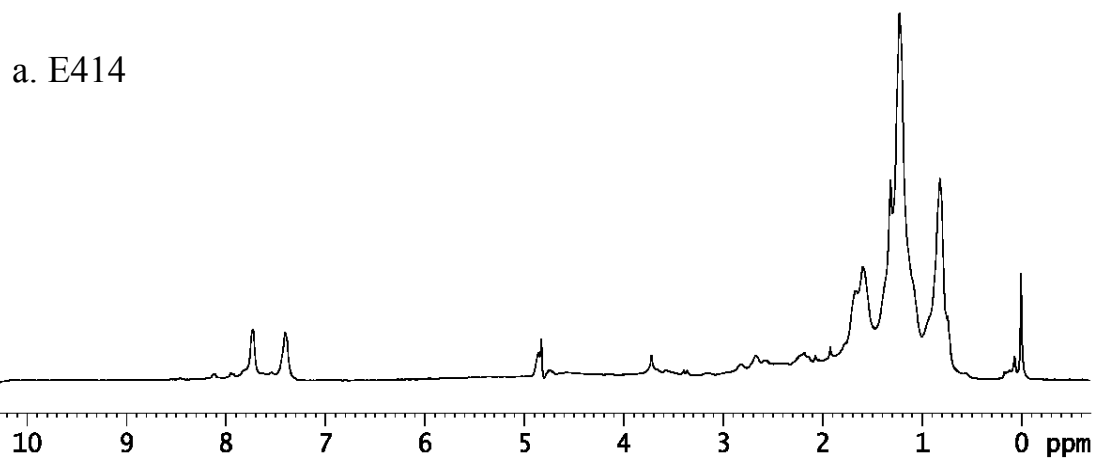


Figure 13-a, b, and c. ¹H NMR presaturation spectra of extractions from two different rain events and a Cape Fear River sample before irradiation.

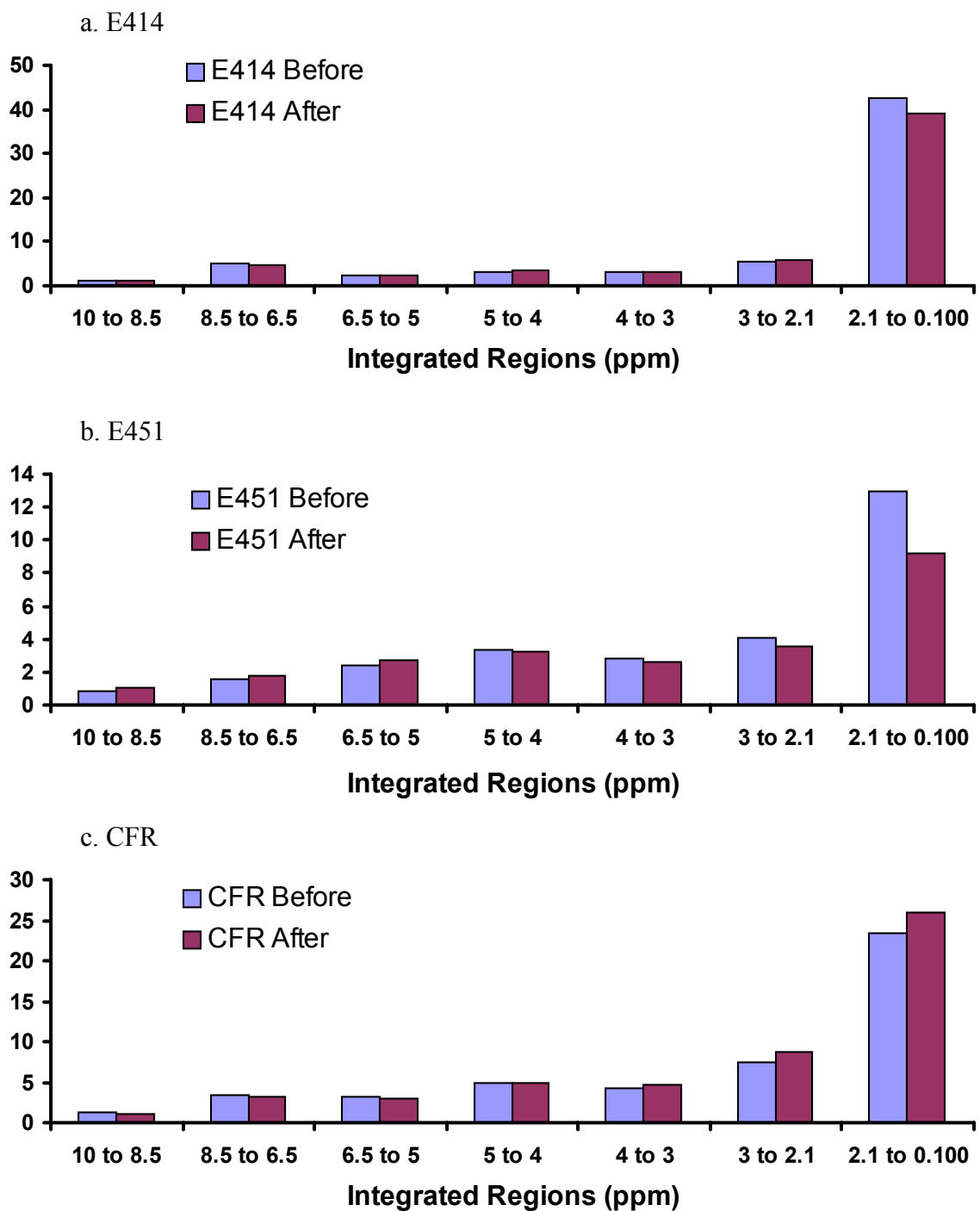


Figure 14-a, b, and c. Before and after irradiation $^1\text{H-NMR}$ integrated regions for two rain events and a natural water sample. CFR = Cape Fear River.

proposed in marine humics (Del Vecchio et al 2002).

The Cape Fear River shows a decrease in $^1\text{H-NMR}$ signal from the region 10 to 5 ppm, no change from 5 to 4 ppm, and an increase in $^1\text{H-NMR}$ signal from 4 to 0.100 ppm. This suggests that during irradiation aromatic protons were lost, suggesting humic degradation of aromatic regions, while the aliphatic proton integration increased, suggesting humification. This was opposite to what was found for rainwater.

Loss of CDOM from rainwater after irradiation was also observed through spectral subtraction for E451. E451's before, after, and spectral subtraction spectra were also compared (Figure 15). The before spectra showed that E451 contained mostly material in the aliphatic region. The spectral subtraction displayed significant loss of material in the aliphatic region. In contrast to the rain samples, the spectral subtraction of the Cape Fear River sample showed no loss in the aromatic region (Figure 16), but significant loss of $^1\text{H-NMR}$ signal in the aliphatic region. This suggests humification in the aliphatic region.

Correlation analysis was performed on the sum of NMR integral regions with other rainwater analytes (DOC, Abs, fluorescence) in order to evaluate patterns of variation between these components. The DOC, absorbance coefficients, and fluorescence surface volume values from 125 rain events were all strongly correlated to each other ($P < 0.001$). In contrast, no correlation was found between the sum of NMR integral regions and DOC, Abs. Coeff. (300nm), Abs. Coeff. (350nm), or surface volume values from the entire fluorescence scan for the five rain events studied by NMR.

Fluorescence was measured on the initial rainwater and on the C_{18} cartridge nonretained eluent and 60% of the initial fluorescence was found in the unretained eluent.

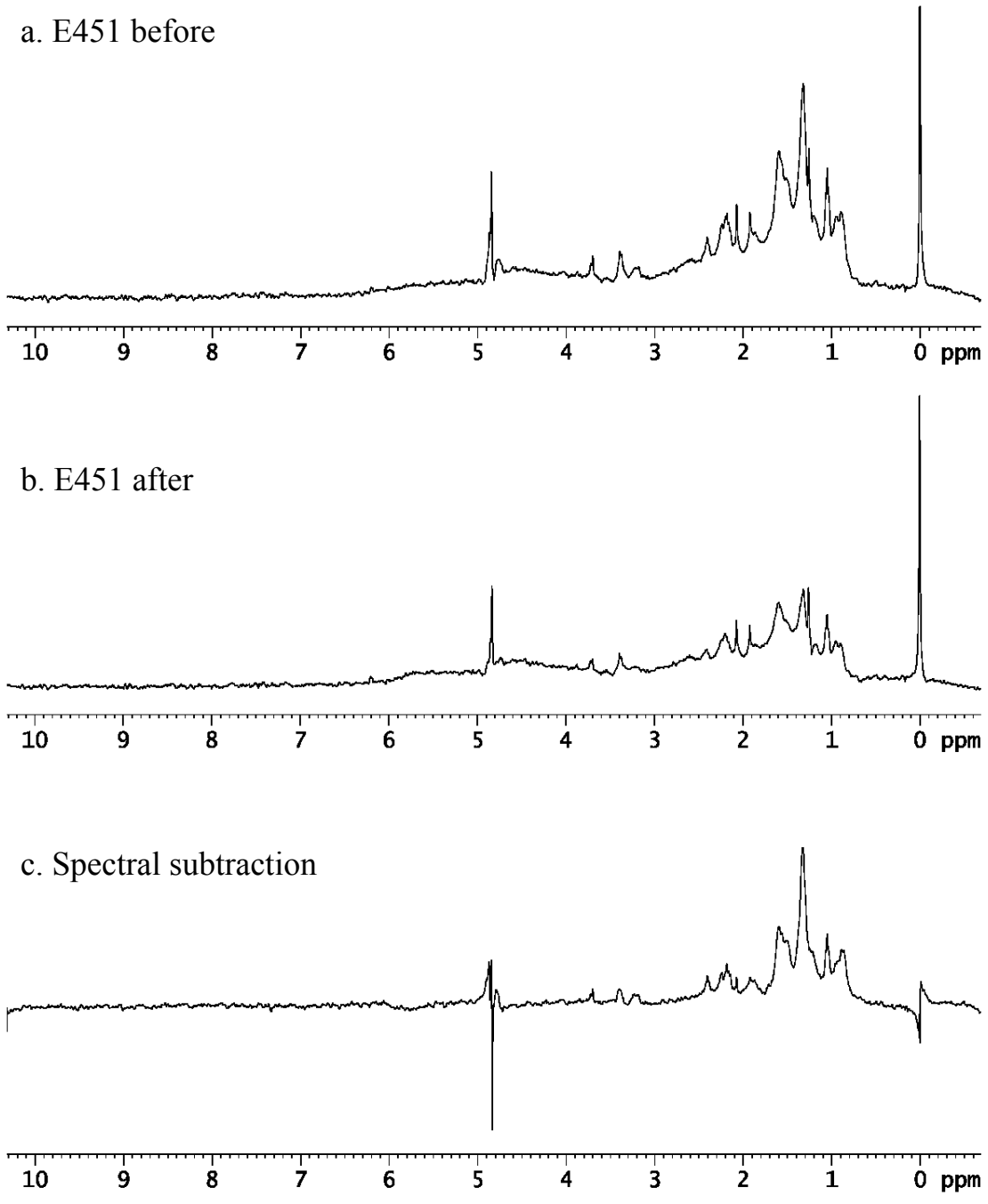


Figure 15-a, b, and c. ^1H NMR presaturation spectra of rain event E451 before/after 12 hour irradiation and the difference between the two.

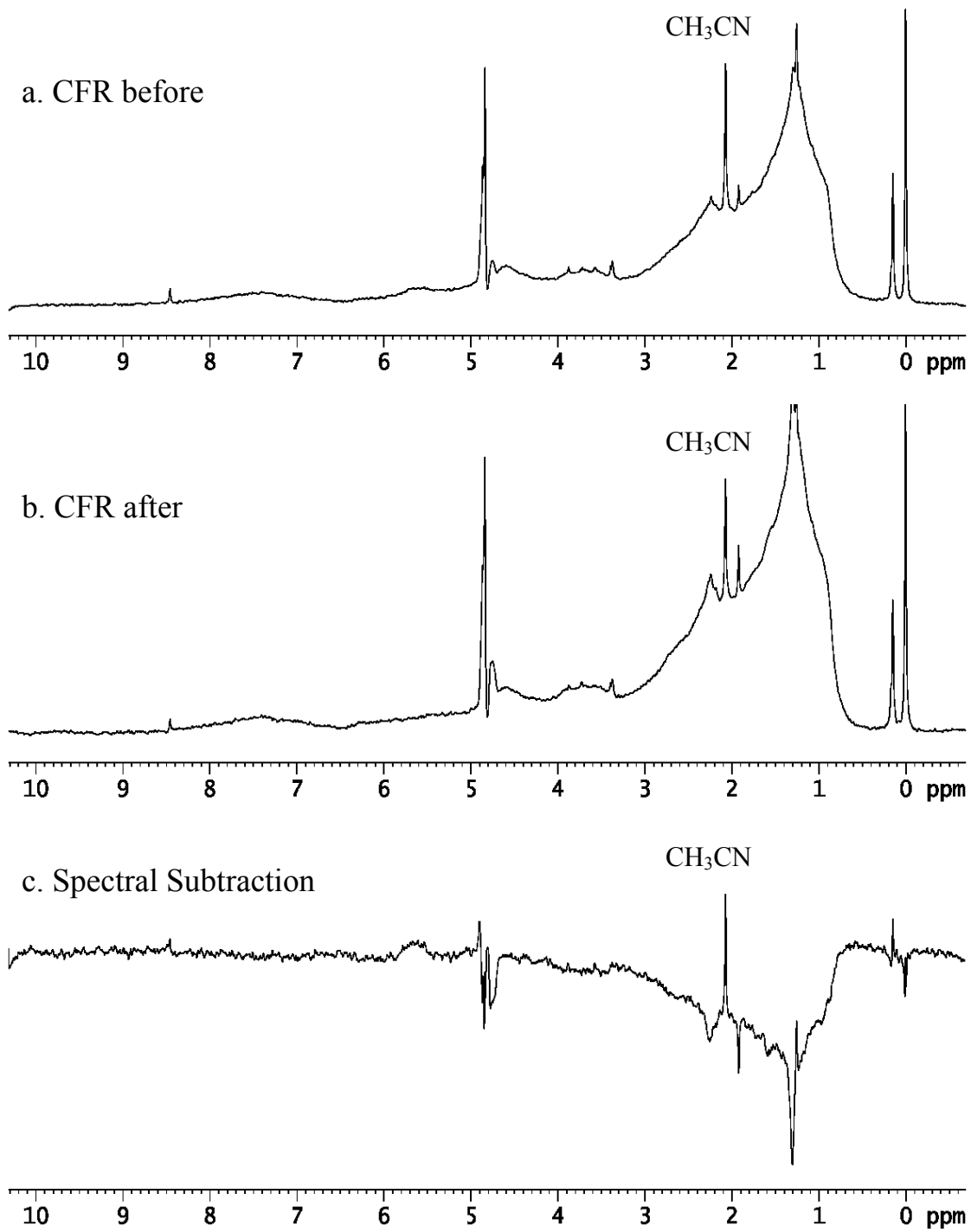


Figure 16-a, b, and c. ¹H NMR presaturation spectra of a Cape Fear River water sample before/after 12 hour irradiation and the difference between the two.

The fluorescence was not altered as it passed through the C₁₈ cartridge, as evidence by the similar, but smaller, relative fluorescence concentrations for the eluent vs. the initial sample. In addition, when Milli-Q was passed through the cartridges no fluorescent bleed-off was found in the Milli-Q eluent. This suggested that the C₁₈ cartridge extracted 40% of the fluorescent CDOM. However, when the CH₃CN extract was reconstituted in Milli-Q, the sample showed no fluorescence, suggesting that extracted fluorescent material was not eluted from the C₁₈ cartridge using this method.

Thus, solid phase cartridge extracted nonfluorescent hydrophobic dissolved organic matter, which explains why there is no correlation between fluorescence and ¹H-NMR integration in these samples. The ¹H-NMR experiments results showed that we were looking primarily at material in the aliphatic region, which does not have strong UV and fluorescent absorbencies. In addition, the extracted material must be a minor component of the DOC based on the poor correlations between DOC and the NMR integrals, as well as the single experiment that measured a DOC recovery of only 15% from E451.

In summary, all rain samples had CDOM, and the fluorescence and absorbance properties of rainwater CDOM are similar to river surface waters in the same region. However, the C/N ratio, photochemical degradation experiments and NMR spectra indicated that there are compositional differences between rainwater and surface waters. CFR CDOM had higher molecular weight and higher C/N ratios, suggesting this material was less volatile and had undergone greater amount of bacterial degradation than rainwater CDOM.